Electronic Supplementary Material (ESI) for Dalton Transactions.

Supporting Information

Redox–state Dependent Activation of Silanes and Ammonia with Reverse Polarity ($PC_{carbene}P$)Ni Complexes: Electrophilic vs. Nucleophilic Carbenes

Etienne A. LaPierre, Warren E. Piers*, Chris Gendy

University of Calgary, Department of Chemistry, 2500 University Drive N.W., Calgary, Alberta, Canada, T2N 1N4.

Contents

Experimental Details

General Considerations. Storage and manipulation of all compounds were performed under an argon atmosphere either in a IT glove box or using a double manifold high vacuum line using standard techniques. Passage of argon through an OxisorBW scrubber (Matheson Gas Products) removed any residual oxygen and moisture. Toluene, hexanes, pentane and tetrahydrofuran were dried and purified using a Grubbs/Dow solvent purification system and stored in 500 mL thick-walled glass vessels over sodium/benzophenone ketal or CaH_2, and distilled under reduced pressure. C_6D_6 and THF-d_8 were dried over sodium/benzophenone ketal, CD_2Cl_2 was dried over CaH_2. All dried solvents were degassed and vacuum distilled prior to use. Anhydrous ammonia was purchased from Air Liquide and purified by condensation on sodium leading to an amber electrolyte. All other reagents were purchased from Sigma-Aldrich and used as received. ^1H and ^{13}C NMR spectrometry chemical shifts were referenced to residual proteo-solvent resonances and naturally abundant ^{13}C resonances for all deuterated solvents. ^{15}N NMR experiments were referenced to $NH_{3(l)}$ at 0 ppm. All other heteronuclear NMR spectrum were referenced externally to IUPAC standards. Chemical shift assignments are based on ^1H, $^{13}C\{^1H\}$, $^{31}P\{^1H\}$, $^{19}F\{^1H\}$, ^1H- ^{13}C-HSQC and ^1H- ^{13}C-HMBC NMR experiments performed on Bruker Ultrashield 400, Ascend-500 or Avance-600 MHz spectrometers. **1**,[1] PhINTs[2] and $ONMePh_2$[3] were prepared per literature procedures. Electrochemical measurements were performed using a CH instruments electrochemical workstation in a drybox under an atmosphere of argon. GC/MS were performed using an Agilent 7890B GC equipped with an Agilent 5977A MSD. All elemental analyses were obtained by the Instrumentation Facility of the Department of Chemistry, University of Calgary. Diffraction patterns were collected with Cu Kα radiation on a Bruker Smart diffractometer equipped with Apex II detector, fixed-CHI goniometer, and sealed-tube (Cu) source or with Mo Kα radiation on a Nonius Kappa CCD diffractometer.

Synthesis of Complex 2

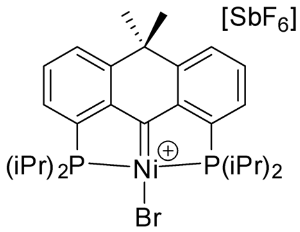

A solution of 200 mg (0.346 mmol) of **1** in 4 mL of DCM was prepared in a 20 mL scintillation vial. To the solution was added 165 mg (0.346 mmol) of [CPh$_3$][SbF$_6$], resulting in the immediate color change to dark green. The solution was allowed to stand overnight and then layered with 15 mL *n*-pentane and cooled to -30 ºC for 2 days. The resulting green-blue needles were separated from the mother liquor, dried *in vacuo*, and washed with 2x10 mL *n*-pentane to yield the title compound as an analytically pure crystalline solid. Crystals grown in this fashion were suitable for single crystal X-ray diffraction studies.

Yield: 270 mg, 0.332 mmol, 96%
^{31}P NMR (203 MHz, Methylene Chloride-*d*$_2$) δ 71.85.

^{1}H NMR (500 MHz, Methylene Chloride-*d*$_2$) δ 8.63 – 8.29 (m, Ar-**H**, 2H), 7.99 (dt, *J* = 7.9, 1.1 Hz, Ar-**H**, 2H), 7.96 – 7.81 (m, Ar-**H**, 2H), 3.16 (m, P-C**H**(CH$_3$)$_2$, 4H), 1.78 (s, C(C**H**$_3$)$_2$, 6H), 1.43 (m, P-CH(C**H**$_3$)$_2$, 24H).

^{13}C NMR (126 MHz, Methylene Chloride-*d*$_2$) δ 250.79 (t, *J* = 9.6 Hz, Ni=**C**), 154.05 (t, *J* = 19.1 Hz, **C$_{\mathbf{Aryl}}$**), 151.14 (t, *J* = 6.2 Hz, **C$_{\mathbf{Aryl}}$**), 141.22 (t, *J* = 16.1 Hz, **C$_{\mathbf{Aryl}}$**), 139.83 (t, *J* = 3.3 Hz, **C$_{\mathbf{Aryl}}$**), 132.52 (**C$_{\mathbf{Aryl}}$**), 132.40 (**C$_{\mathbf{Aryl}}$**), 42.37 (**C**(CH$_3$)$_2$), 28.82 (C(**C**H$_3$)$_2$), 25.22 (t, *J* = 12.2 Hz, P-**C**H(CH$_3$)$_2$), 18.21 (P-CH(**C**H$_3$)$_2$), 17.45, (P-CH(**C**H$_3$)$_2$) .

Elemental Analysis: Calcd (%): C 41.37; H 4.96. Found (%): C 41.43; H 5.07

Synthesis of Complex 2$_{\mathbf{red}}$

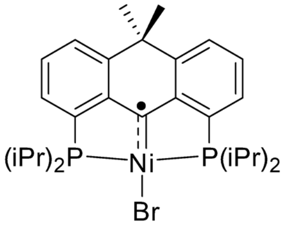

To 3 mL of a THF solution of 100 mg (0.123 mmol) of **2** was added 25 mg (0.129 mmol, 1.05 eq) of solid cobaltocene. An immediate color change from blue-green to blue-red was noted. The solvent was removed *in vacuo* and the dark blue residue was extracted with 5 mL n-pentane from the yellow cobaltocenium salt. The suspension was filtered through a 0.2 µm PTFE syringe filter, and cooled to -30 ºC to yield analytically pure **3** as dichroic blue-red X-ray quality crystals.

Yield: 36 mg, 0.062 mmol, 51%

μ_{eff}=1.76 μ_{B} (Evan's Method)

Elemental Analysis: Calcd (%): C 58.27; H 6.99. Found (%): C 58.26; H 6.86.

Synthesis of 3_{O}

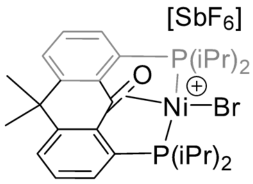

To a cold (-30 °C) 4 mL of a DCM solution containing **2** (50 mg, 0.061 mmol) was added 13mg (0.065 mmol, 1.05 eq.) of $ONMePh_2$ as a solid. The solution immediately became dark brown. The solution was layered with 15 mL n-pentane, and cooled to -30°C for two days. The mother liquor was separated by decantation. The brown residue was dissolved in minimal DCM and layered with 15 mL n-pentane and cooled to -30 °C for a further 2 days. The resulting brown residue was isolated by decantation and dried under vacuum. X-ray quality crystals were grown by vapor diffusion of n-pentane to a saturated fluorobenzene (~4 mg/mL) solution at ambient temperature.

IR ν=1571 cm^{-1}

Yield 39 mg, 0.047 mmol, 76%

^{31}P NMR (203 MHz, Methylene Chloride-d_2) δ 30.94.

^{1}H NMR (500 MHz, Methylene Chloride-d_2) δ 8.11 – 7.85 (m, 4H, Ar-**H**), 7.53 (m, 2H), 2.72 – 2.62 (m, P-C**H**(CH_3)$_2$, 2H), 2.49 (m, P-C**H**(CH_3)$_2$, 2H), 2.03 (s, C(C**H**$_3$)$_2$, 3H), 1.72 (dd, *J* = 8.2 Hz, P-CH(C**H**$_3$)$_2$, 6H), 1.63 (s, C(C**H**$_3$)$_2$, P-CH(C**H**$_3$)$_2$, 6H), 1.28 (m, P-CH(C**H**$_3$)$_2$, 12H).

^{13}C NMR (126 MHz, Methylene Chloride-d_2) δ 182.84 (**C**=O), 152.59 (**C$_{Aryl}$**), 138.19 (**C$_{Aryl}$**), 137.31 (t, *J* = 3.4 Hz, **C$_{Aryl}$**), 131.81 (**C$_{Aryl}$**), 130.92 (**C$_{Aryl}$**). 127.18 (t, *J* = 13.9 Hz, **C$_{Aryl}$**), 40.99 (**C**(CH_3)$_2$), 34.61 (C(**C**H$_3$)$_2$), 28.49 (C(**C**H$_3$)$_2$), 26.74 (t, *J* = 10.2 Hz, P-**C**H(CH_3)$_2$), 24.84 (t, *J* = 12.1 Hz, P-**C**H(CH_3)$_2$), 19.79 (P-CH(**C**H$_3$)$_2$), 18.83 (P-CH(**C**H$_3$)$_2$), 18.29 (P-CH(**C**H$_3$)$_2$), 17.15 (P-CH(**C**H$_3$)$_2$).

Elemental Analysis: Calcd (%): C 40.57; H 4.86. Found (%): C 40.85; H 5.04; N 0.04.

Synthesis of 3_{NTs}

To a cold (-30 °C) 4 mL of a DCM solution containing **2** (60 mg, 0.074 mmol) was added 28 mg (0.078 mmol, 1.05 eq.) of $ONMePh_2$ as a solid. The solution immediately became dark brown. The solution was layered with 15 mL n-pentane, and cooled to -30°C for two days. The mother liquor was separated by decantation. The brown residue was dissolved in minimal THF and layered

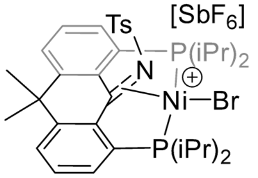

with 15 mL n-pentane and cooled to -30 ºC for a further 2 days. The resulting brown residue was isolated by decantation and dried under vacuum. X-ray quality crystals were grown by vapor diffusion of n-pentane in to a saturated fluorobenzene (~4 mg/mL) solution at ambient temperature.

Yield:45 mg, 0.0458 mmol, 62%

IR ν=1595 cm^{-1}

^{31}P NMR (243 MHz, Methylene Chloride-*d*$_2$) δ 40.47.

^{1}H NMR (600 MHz, Methylene Chloride-*d*$_2$) δ 7.97 – 7.86 (m, Ar-**H**(ligand), 4H), 7.53 (m, Ar-**H**(ligand), 2H), 7.42 (d, *J* = 8.1 Hz, Ar-**H**, Ts, 2H), 7.24 (d, *J* = 8.1 Hz, Ar-**H**, Ts, 2H), 2.95 – 2.81 (m, P-C**H**(CH$_3$)$_2$, 4H), 2.36 (s, Ts C**H$_3$**, 3H), 1.94 (s, C(C**H**$_3$)$_2$, 3H), 1.82 – 1.68 (m, 6H), 1.59 (dd, *J* = 7.7 Hz, P-CH(C**H**$_3$)$_2$ 6H), 1.36 (s, C(C**H**$_3$)$_2$, 3H), 1.32 (dd, *J* = 8.1 Hz, P-CH(C**H**$_3$)$_2$, 6H), 1.23 (dd, *J* = 7.5 Hz, P-CH(C**H**$_3$)$_2$, 6H).

^{13}C NMR (151 MHz, Methylene Chloride-*d*$_2$) δ 149.27 (t, *J* = 4.2 Hz, **C$_{Aryl}$**), 147.04 (**C$_{Aryl}$**), 139.91 (**C**=N), 138.45 (t, *J* = 6.6 Hz, **C$_{Aryl}$**), 136.16 (**C$_{Aryl}$**), 135.18 (t, *J* = 3.4 Hz, **C$_{Aryl}$**), 131.50 (**C$_{Aryl}$**), 130.72 (**C$_{Aryl}$**), 130.27 (**C$_{Aryl}$**), 128.74 (t, *J* = 14.8 Hz, **C$_{Aryl}$**), 127.61 (**C$_{Aryl}$**), 41.25 (**C**(CH$_3$)$_2$), 35.84 (C(**C**H$_3$)$_2$), 28.79 (m, 2C, P-**C**H(CH$_3$)$_2$, 4.6 Hz), 28.07 (C(**C**H$_3$)$_2$), 21.84 (NTs **C**H$_3$), 20.37 (P-CH(**C**H$_3$)$_2$), 19.45 (P-CH(**C**H$_3$)$_2$), 19.39 (P-CH(**C**H$_3$)$_2$), 18.64 (P-CH(**C**H$_3$)$_2$).

Elemental Analysis: Calcd (%): C 42.80; H 4.82; N 1.43. Found (%): C 42.93; H 4.61; N 1.71.

Synthesis of Complex 4

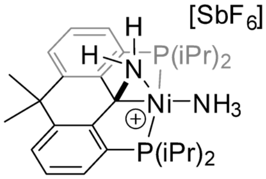

To a 5 mL thick walled glass vessel containing fine ground **2** (50 mg, 0.061 mmol), was condensed 1.5 mL of freshly distilled liquid ammonia at -78ºC. An immediate color change to red-purple was noted. The ammonia was removed *in vacuo*. The residue was extracted with 5 mL fluorobenzene and the resulting solution was filtered through a 0.2 µm PTFE syringe filter to remove a white precipitate. The solution was then layered with n-pentane to yield fuchsia crystals of the title compound. Crystals suitable for X-ray diffraction were grown from 1:3 DCM/pentane at -30 ºC.

Yield: 27 mg, 0.035 mmol, 58%

^{15}N NMR (51 MHz, THF-d_8) δ 29.85 (t, J = 9.8 Hz, C-**N**H_2-Ni), -52.59(s, Ni-**N**H_3).

^{31}P NMR (203 MHz, THF-d_8) δ 41.56.

^{1}H NMR (500 MHz, THF-d_8) δ 7.65 (d, J = 7.7 Hz, Ar-**H**, 2H), 7.60 (m, Ar-**H**, 2H), 7.47 (t, J = 7.7 Hz, Ar-**H**, 2H), 3.79 (s, N**H**$_\mathbf{2}$, 2H), 2.95 – 2.80 (m, P-C**H**(CH_3)$_2$, 2H), 2.45 – 2.30 (m, P-C**H**(CH_3)$_2$, 2H), 1.86 (s, C(C**H**$_3$)$_2$, 3H), 1.58 (s, C(C**H**$_3$)$_2$, 3H), 1.53 (t, J = 4.1 Hz, N**H**$_\mathbf{3}$, 3H), 1.49 – 1.41 (m, P-CH(C**H**$_3$)$_2$, 12H), 1.28 (dd, J = 7.1 Hz, P-CH(C**H**$_3$)$_2$, 6H), 0.92 (dd, J = 7.3 Hz, P-CH(C**H**$_3$)$_2$, 6H).

^{13}C NMR (126 MHz, THF-d_8) δ 149.41 (t, J = 20.2 Hz, **C**$_\mathbf{Aryl}$), 145.10 (t, J = 7.8 Hz, **C**$_\mathbf{Aryl}$), 133.89 – 133.43 (m, **C**$_\mathbf{Aryl}$), 128.73 (**C**$_\mathbf{Aryl}$), 127.86 (**C**$_\mathbf{Aryl}$), 125.66 (**C**$_\mathbf{Aryl}$), 63.53 (br s, N-**C**-Ni), 39.02 (**C**(CH_3)$_2$), 34.18 (C(**C**H_3)$_2$), 25.91 (t, (P-**C**H(CH_3)$_2$, J = 6.1 Hz), 24.50 (C(**C**H_3)$_2$), 18.50 (t, P-CH(**C**H_3)$_2$, J = 3.6 Hz), 18.40 (t, P-CH(**C**H_3)$_2$, J = 3.3 Hz), 17.72 (P-CH(**C**H_3)$_2$), 17.43 (t, P-CH(**C**H_3)$_2$, J = 3.5 Hz). Remaining peak for (P-**C**H(CH_3)$_2$) unresolved from solvent peak.

Elemental Analysis: Calcd (%): C 43.90; H 5.92; N 3.66. Found (%): C 44.39; H 5.68; N 3.32.

Synthesis of Complex 6

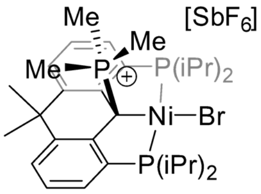

To 0.7 mL PhF solution containing 30 mg (0.037) of **2** in a 20 mL vial was added excess PMe_3 (1 drop, *via* Pasteur pipette). An immediate quenching of the intense blue-green color of **2**, leading to an orange-yellow solution. The solution was layered with 9 mL of *n*-pentane and cooled to -30°C for two days. The resulting orange-yellow needles were separated from the mother liquor by decantation, washed with *n*-pentane and dried under vacuum. Crystals grown in this fashion were suitable for single crystal X-ray diffraction studies.

Yield: 27 mg, 0.0303 mmol, 82%

^{31}P NMR (203 MHz, Methylene Chloride-d_2) δ 37.28 (2P, Ligand), 34.29 (1P, **P**Me_3).

^{1}H NMR (500 MHz, Methylene Chloride-d_2) δ 7.75 (d, J = 7.1 Hz, Ar-**H**, 2H), 7.62 – 7.43 (m, Ar-**H**, 4H), 2.81 (m, P-C**H**(CH_3)$_2$, 2H), 2.76 – 2.67 (m, P-C**H**(CH_3)$_2$, 2H), 1.82 (s, C(C**H**$_3$)$_2$, 3H), 1.73

– 1.60 (m, P-CH(C**H**$_3$)$_2$, and P(C**H$_3$**)$_3$ 21H), 1.58 (s, C(C**H**$_3$)$_2$,3H), 1.30 (dd, *J* = 8.7, 7.1 Hz, P-CH(C**H**$_3$)$_2$, 6H), 1.15 (dd, *J* = 7.2 Hz, , P-CH(C**H**$_3$)$_2$, 6H).

^{13}C NMR (126 MHz, Methylene Chloride-*d*$_2$) δ 145.57 (td, *J* = 17.1, 6.2 Hz, **C$_{Aryl}$**), 144.54 (dd, *J* = 6.5 Hz, **C$_{Aryl}$**), 133.59 (m, **C$_{Aryl}$**), 130.76 (d, *J* = 5.0 Hz, **C$_{Aryl}$**), 130.00 (d, *J* = 4.4 Hz, **C$_{Aryl}$**), 128.94 – 128.25 (m, **C$_{Aryl}$**), 47.27 – 44.57 (m, P-**C**-Ni), 38.66 (d, *J* = 3.5 Hz, **C**(CH$_3$)$_2$), 35.13 (d, *J* = 6.7 Hz, C(**C**H$_3$)$_2$), 32.70 (d, *J* = 5.2 Hz, C(**C**H$_3$)$_2$), 28.04 (t, *J* = 12.0 Hz, P-**C**H(CH$_3$)$_2$), 25.85 (t, *J* = 11.1 Hz, P-**C**H(CH$_3$)$_2$), 19.76 (P-CH(**C**H$_3$)$_2$), 18.79 (P-CH(**C**H$_3$)$_2$), 18.73 (P-CH(**C**H$_3$)$_2$), 17.77 (P-CH(**C**H$_3$)$_2$), 12.47 (d, *J* = 51.0 Hz, P(**C**H$_3$)$_3$).

Elemental Analysis: Calcd (%): C 41.88; H 5.56. Found (%): C 41.53; H 5.76

Isolation of Crystals of 4 and 5

10 mg of **2** was dissolved in 0.5 mL DCM in a J-Young NMR tube. The solution was degassed by one freeze-pump-thaw cycle and placed under one atmosphere of $NH_{3(g)}$. The solution immediately changed color to deep red-purple. Volatiles were removed *in vacuo* and the residue was reconstituted in 1 mL DCM, filtered through a 0.2 µm PTFE syringe filter, layered with *n*-pentane and cooled to -30 ºC for 2 days. The resulting fuchsia crystals (<1 mg) of **4** were manually separated from an orange oil, and the X-ray diffraction pattern collected. The oil was reconstituted in C_6D_6 and it was confirmed to be a mixture of **5** and an unidentified product. Vapor diffusion of pentane into this sample led to the precipitation of an orange oil. This orange oil was suspended in pentane and refrigerated at -30ºC for 6 weeks, leading to orange plate crystals (<1 mg).

Procedure for catalytic hydrodefluorination with 2

In a one dr. vial **2** 5.0 mg (0.0062 mmol) of **2** was dissolved in ca. 0.6 mL of α,α,α-trifluorotoluene and 6.0 mg (0.0083 mmol) of $K[B(C_6F_5)_4]$ was added. The mixture was agitated for 30 min and then filtered using a 0.2 μm PTFE syringe filter and the filtrate transferred to a J-Young NMR tube $^{31}P\{^1H\}$ NMR of this mixture showed 1 product identical to **2**, while $^{19}F\{^1H\}$ NMR showed the incorporation of $[B(C_6F_5)_4]^-$. To this solution was added 100 μL silane (0.652 mmol $HSiMe_2Ph$ or 0.626 mmol $HSiEt_3$). The reaction was allowed to stand for 30 min and then analysed by $^{19}F\{^1H\}$ and $^{31}P\{^1H\}$ spectrometry, showing no reaction. The reaction mixture was then heated to 80 °C for 30 min ($HSiMe_2Ph$) or 1 h ($HSiEt_3$), resulting in a color change to pale pink and the formation of a black precipitate (presumably Ni black). $^{19}F\{^1H\}$ and $^{11}B\{^1H\}$ NMR spectra suggest that the borate counter ion is still present, while the $^{31}P\{^1H\}$ NMR spectrum shows no trace of **1** or **2**. The tube was returned to the drybox and 50 μL (0.532 mmol) of PhF was added as an NMR standard. The yield of F-Si species was determined by $^{19}F\{^1H\}$ NMR spectrometry (d1=20s). Further heating did not lead to increased F-Si bond formation. GC/MS and ^1H NMR analysis of the reaction mixture show the formation of toluene, only trace toluene was observed when $HSiMe_2Ph$ was used while appx. 1 eq. of toluene per 7 $FSiEt_3$ was detected *via* GC/MS. The difference between the yield of toluene and silylfluoride can be partially explained by the tendency of this substrate to form oligomeric species or reaction with tetrakis(pentafluorophenyl)borate.[4] While F-Si bond formation can be used to estimate TON, typically this number is less (10-20%) than the actual number of C-F bonds broken due to leaching to the borosilicate glass.[5]

Table S1: Catalytic hydrodefluorination of trifluorotoluene with 2

Run	**Silane**	**Eq. Si-F**[a]
1	$HSiPhMe_2$	22
2	$HSiEt_3$	35

[a] Equivalents of F-Si bonds produced per equivalent of **2** assuming no loss of catalyst during filtration

Supplementary Figures

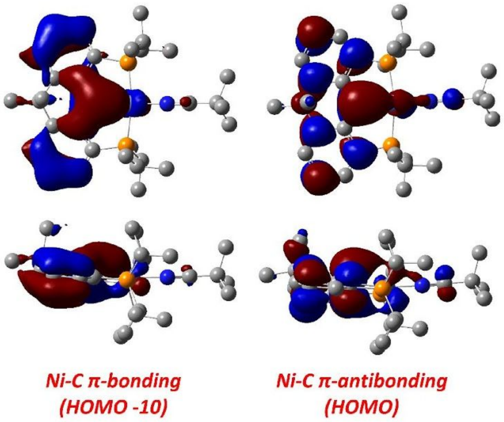

Figure S1. DFT Calculated Molecular Orbitals of II.

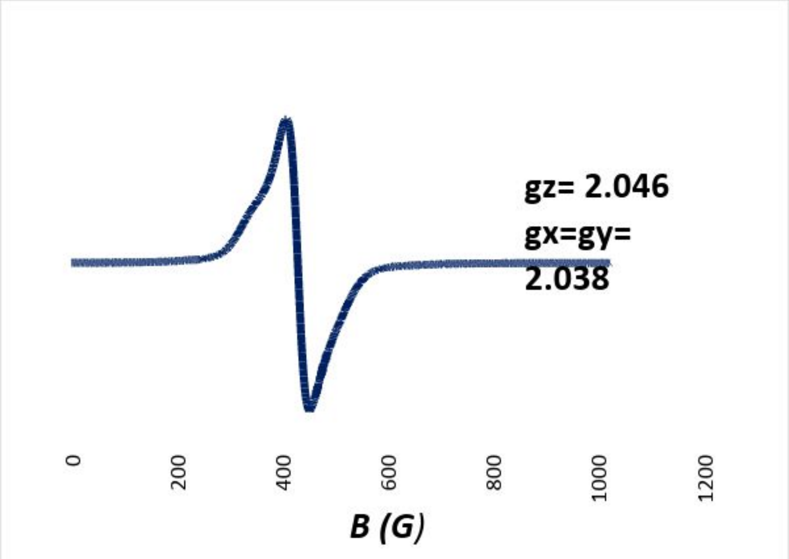

Figure S2. X-Band EPR Spectra of 2_{red} (Toluene glass, 128K)

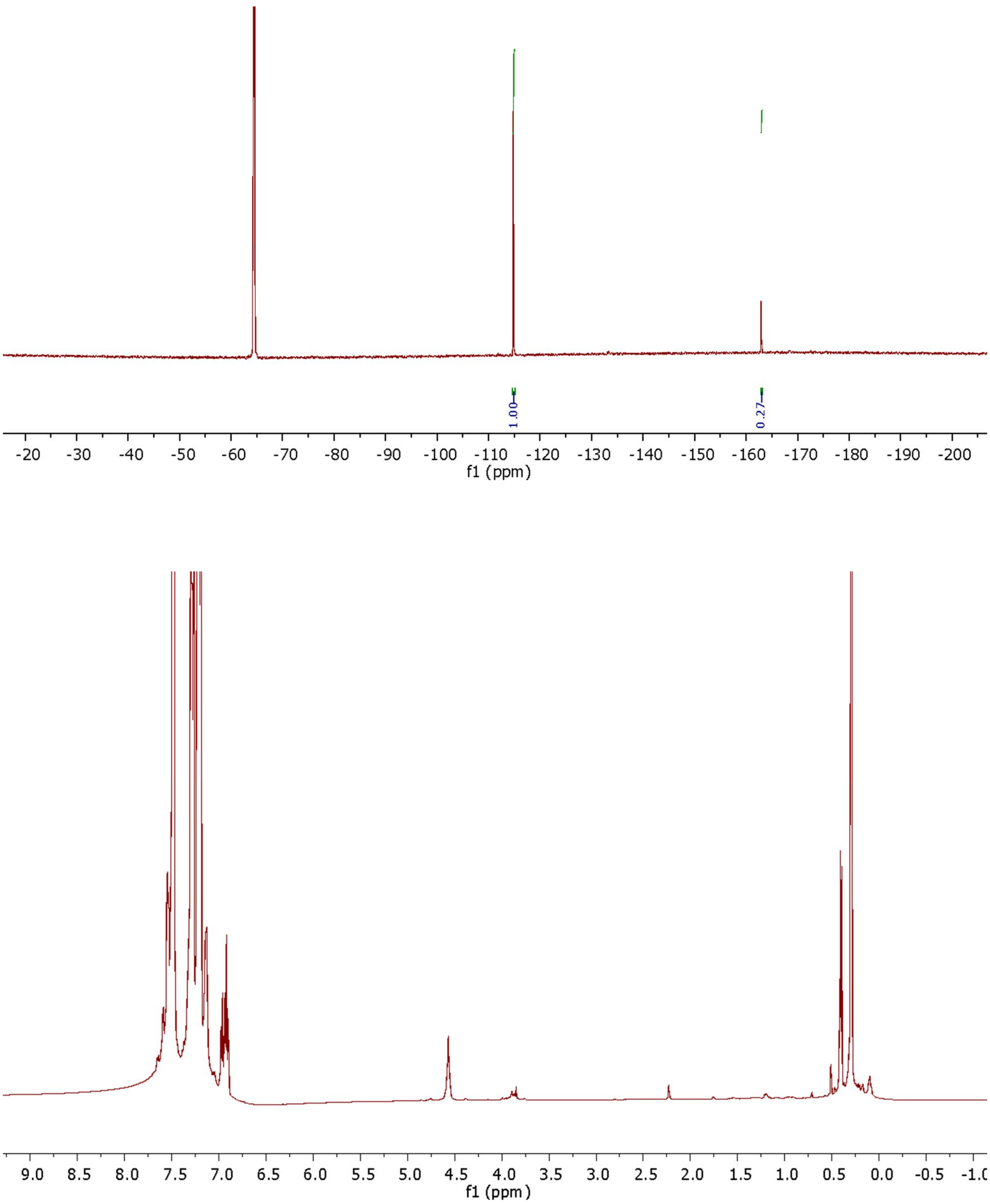

Figure S3: $^{19}F\{^1H\}$ (top) and ^1H NMR Spectra (bottom) of Run 1. FSiMe2Ph (-163 ppm) and toluene (~2.2 ppm) are clearly observable

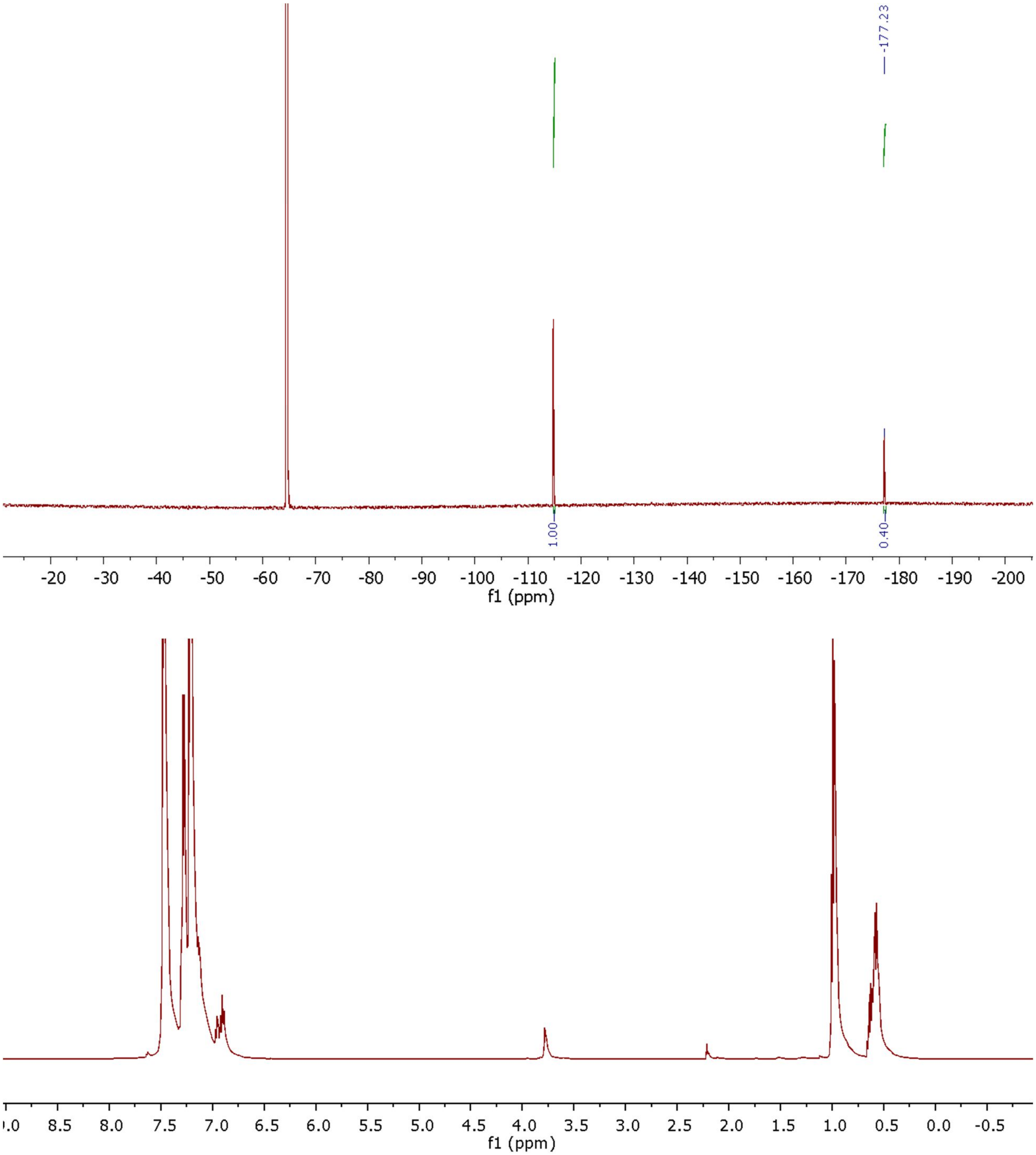

Figure S4: $^{19}F\{^{1}H\}$ (top) and ^{1}H (bottom) NMR Spectra of Run 2. FSiEt3 (-177 ppm) and toluene (~2.2 ppm) are clearly observable

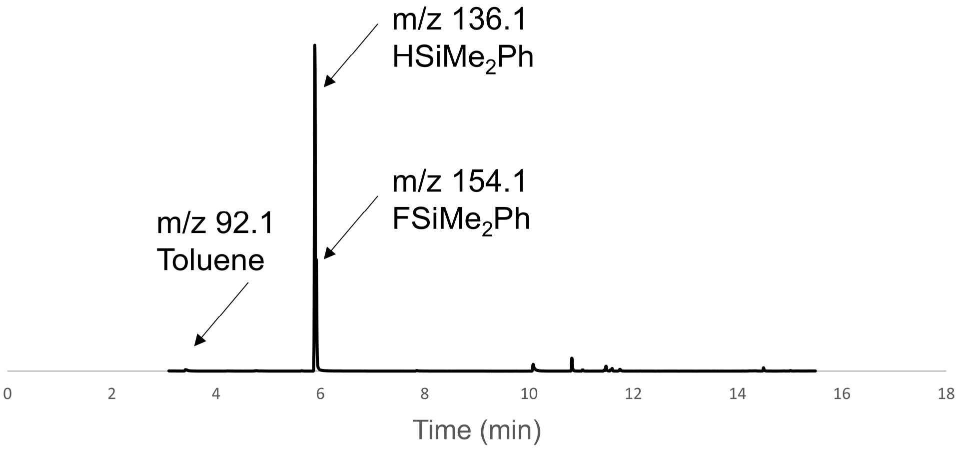

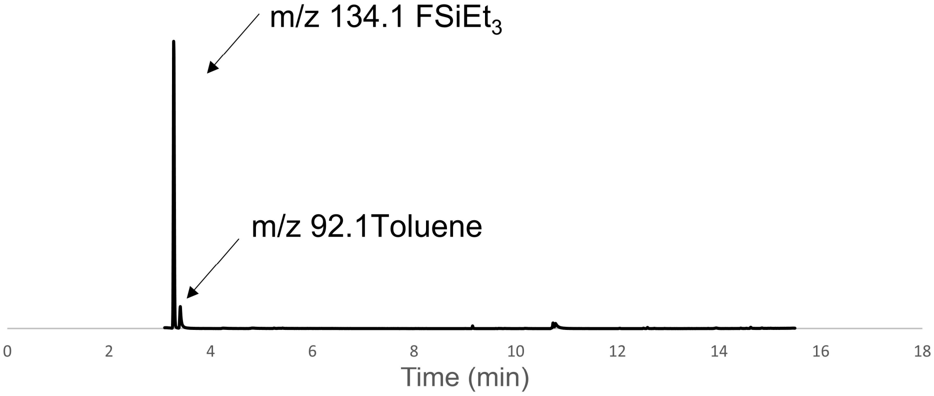

Figure S5: Gas chromatograms of the reaction mixtures of Run 1(top) and Run 2 (bottom)

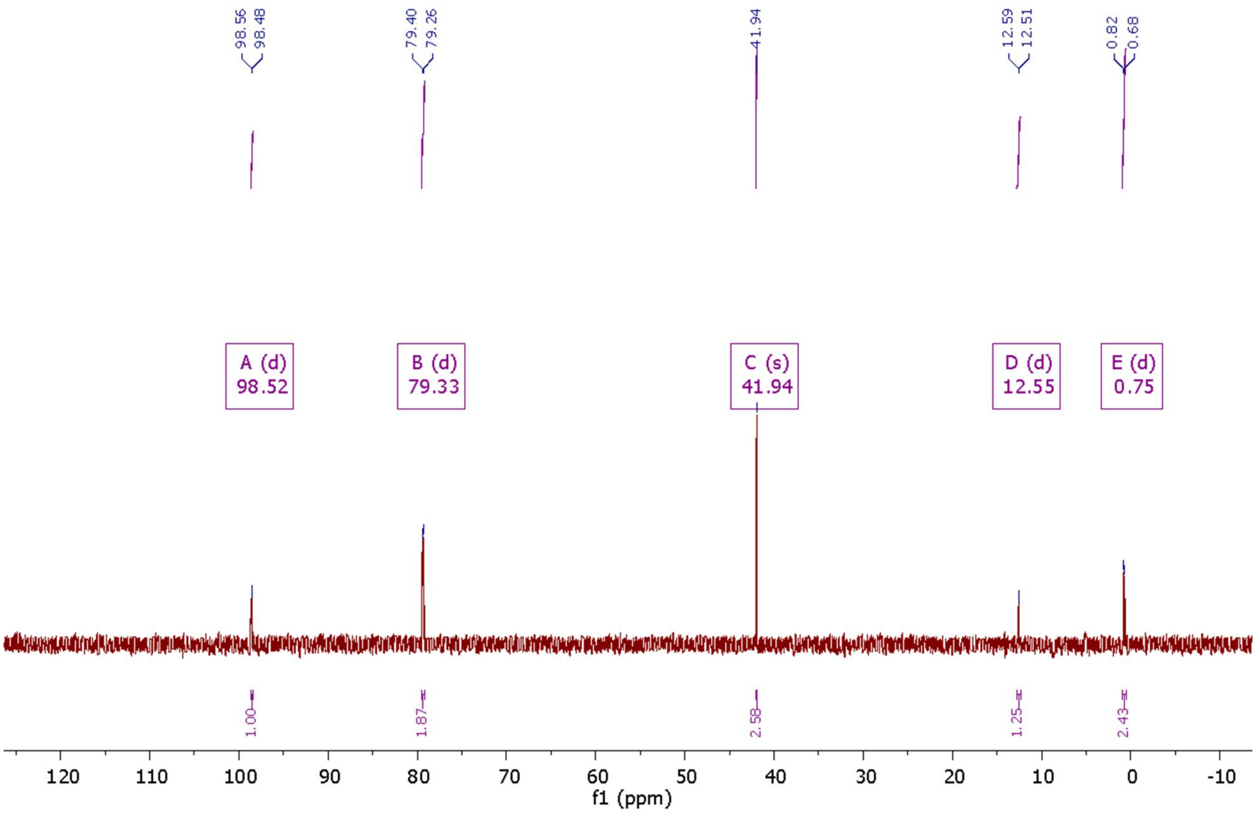

Figure S6. $^{31}P\{^1H\}$ NMR Spectrum of the Reaction of 2 with Ammonia in Solution. Reconstituted in C_6D_6. ^{31}P NMR (203 MHz, Benzene-*d*$_6$) δ 98.52 (d, *J* = 16.3 Hz), 79.33 (d, *J* = 29.0 Hz), 41.94 (4), 12.55 (d, *J* = 16.3 Hz), 0.75 (d, *J* = 28.9 Hz).

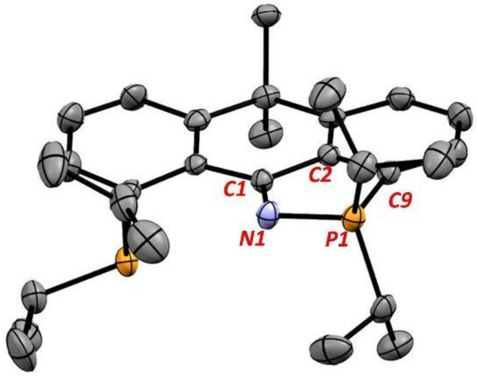

Figure S7. ORTEP diagram for complex 5. Thermal ellipsoids are shown at the 50% probability level. Hydrogen atoms and counter anions are omitted for clarity. Select bond lengths (Å) and angles (degrees) for 4a: N1-C1 1.313(6), N1-P1 1.666(4), C1-C2 1.472(6), C2-C9 1.401(6), C9-P1 1.789(4), C1-N1-P1 109.6(3).

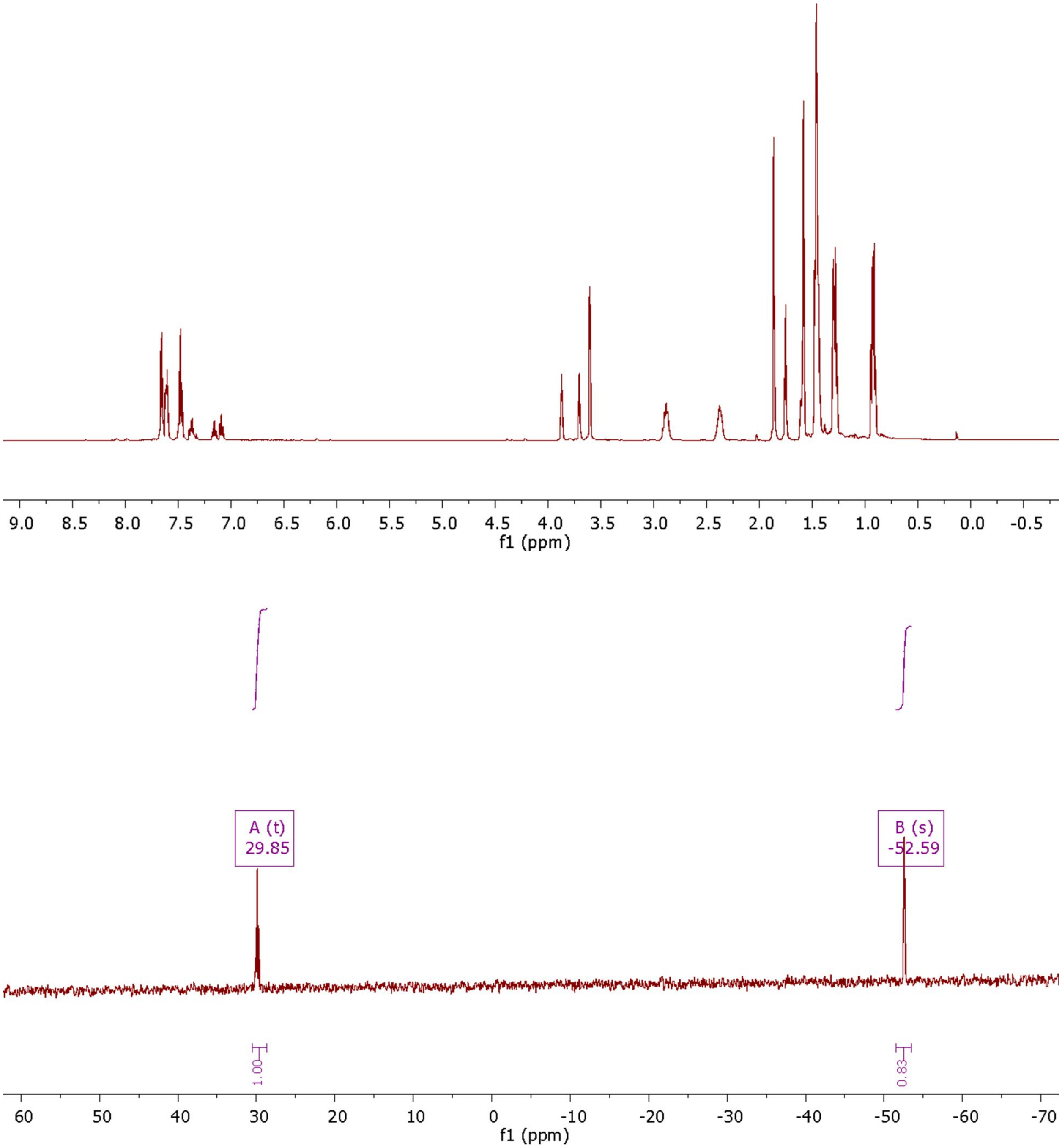

Figure S8. ^{1}H NMR Spectrum (Top) and ^{15}N{^{1}H} NMR Spectrum (Bottom) of ^{15}N-Labelled (98%) 4. Contamination by co-crystallized PhF evident.

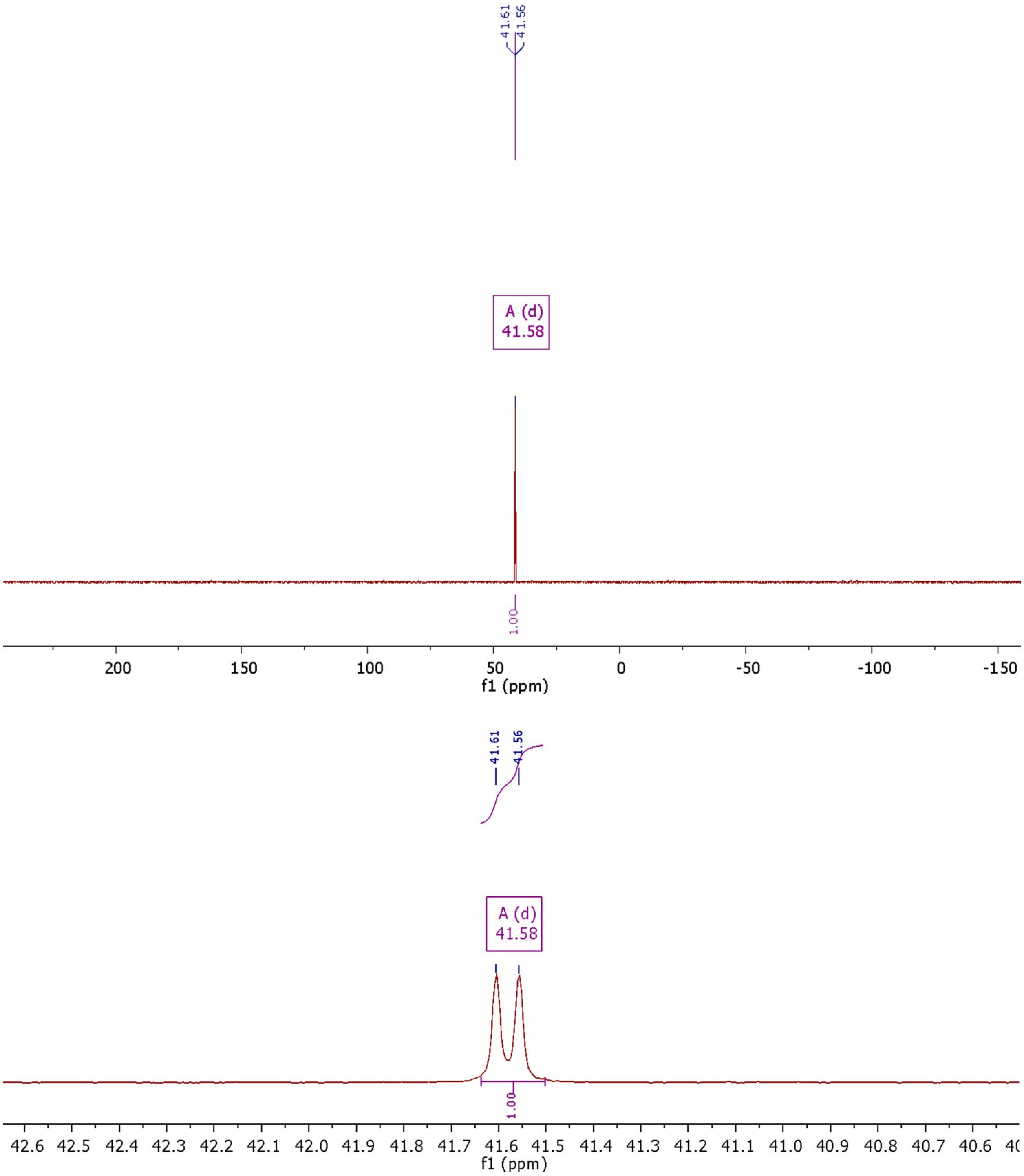

Figure S9. $^{31}P\{^{1}H\}$ **NMR Spectrum** ^{15}N**-Labelled(98%) 4.**

Crystal Data Collection and Refinement Parameters

Table S1. Crystal Data Collection and Refinement Parameters for Complexes 2_x

	2	**2_{red}**
formula	$C_{28}H_{40}BrNiP_2,F_6Sb$	$C_{28}H_{40}BrNiP_2$
fw	812.91	577.16
crystal system	monoclinic	triclinic
space group	$P2_{1/n}$	P-1
a **(Å)**	12.454(11)	11.0190(6)
b **(Å)**	14.888(13)	11.1636(7)
c **(Å)**	18.079(18)	13.0424(8)
α (deg)	90	107.237(2)
β (deg)	95.797(14)	98.206(2)
γ (deg)	90	111.768(2)
V **($Å^3$)**	3335(5)	1364.11(14)
Z	4	2
T **(K)**	173(2)	173(2)
Wavelength (Å)	0.71073	0.71073
ρ_{calcd} ($g \cdot cm^{-3}$)	1.619	1.405
F**(000)**	1624	602
μ (mm^{-1})	2.719	2.307
crystal size, mm^3	0.14×0.13×0.08	0.27×0.26×0.26
transmission factors	0.6763 − 0.7454	0.6172 − 0.7456
θ **range (deg)**	1.776 − 24.999	3.040 − 27.564
data/restraints/param	5828/372/362	6218/0/299
GOF	0.976	1.000
R_1 [$I > 2\sigma(I)$]	0.0422	0.0334
wR_2 [all data]	0.0921	0.0801
residual density, e/$Å^3$	1.052 and -0.870	0.509 and -0.513

Table S2. Crystal Data Collection and Refinement Parameters for Complexes 3_x

	3_O	**3_{NTs}**
formula	$C_{28}H_{40}BrNiOP_2,F_6Sb$[+solvent]	$C_{35}H_{48}BrNNiO_2P_2S,F_6Sb$
fw	828.91	982.10
crystal system	monoclinic	monoclinic
space group	P21/n	P21/c
***a* (Å)**	16.4321(4)	11.7793(5)
***b* (Å)**	14.2612(5)	15.5651(9)
***c* (Å)**	16.6228(5)	20.8787(11)
α (deg)	90	90
β (deg)	110.710(2)	90.523(3)
γ (deg)	90	90
***V* ($Å^3$)**	3643.7(2)	3827.9(3)
Z	4	4
***T* (K)**	173(2)	173(2)
Wavelength (Å)	0.71073	0.71073
ρ_{calcd} ($g \cdot cm^{-3}$)	1.511	1.704
***F*(000)**	1656	1976
μ (mm^{-1})	2.492	2.442
crystal size, mm^3	0.14×0.13×0.03	0.22×0.21×0.05
transmission factors	0.6117 − 0.7456	0.5972 − 0.7456
***θ* range (deg)**	1.938 − 27.511	2.168 − 25.000
data/restraints/param	8301/381/371	6680/0/462
GOF	0.998	1.010
R_1 [$I > 2\sigma(I)$]	0.0450	0.0314
wR_2 [all data]	0.1125	0.0723
residual density, e/$Å^3$	0.816 and -0.637	0.562 and -0.848

Table S3. Crystal Data Collection and Refinement Parameters for 4 and 5

	4	**5**
formula	$C_{28}H_{45}N_2NiP_2,F_6Sb$	$C_{28}H_{40}NP_2,F_6Sb$[+solvent]
fw	766.06	688.30
crystal system	monoclinic	monoclinic
space group	$P_{21/n}$	P21/n
a **(Å)**	10.9965(3)	14.4344(11)
b **(Å)**	16.1517(4)	10.4579(7)
c **(Å)**	18.8351(4)	22.2043(14)
α (deg)	90	90
β (deg)	101.9790(10)	98.505(3)
γ (deg)	90	90
V **($Å^3$)**	3272.49(14)	3315.0(4)
Z	4	4
T **(K)**	173(2)	173(2)
Wavelength (Å)	0.71073	0.71073
ρ_{calcd} ($g \cdot cm^{-3}$)	1.555	1.379
F**(000)**	1560	1400
μ (mm^{-1})	1.553	0.979
crystal size, mm^3	0.28×0.26×0.25	0.18×0.11×0.05
transmission factors	0.6064 − 0.7456	0.5927 − 0.7456
θ **range (deg)**	3.154 − 25.000	2.690 − 25.000
data/restraints/param	5713/0/372	5790/330/353
GOF	1.016	1.052
R_1 [$I > 2\sigma(I)$]	0.0315	0.0432
wR_2 [all data]	0.0812	0.1193
residual density, e/$Å^3$	1.322 and -0.962	0.560 and -0.697

Table S4. Crystal Data Collection and Refinement Parameters for 6

	6
formula	$C_{31}H_{49}BrNiP_3,F_6Sb$[+solvent]
fw	888.98
crystal system	orthorhombic
space group	Fdd2
a **(Å)**	38.776(8)
b **(Å)**	51.519(10)
c **(Å)**	9.2266(18)
α (deg)	90
β (deg)	90
γ (deg)	90
V **(Å^3)**	18432(6)
Z	16
T **(K)**	173(2)
Wavelength (Å)	0.71073
ρ_{calcd} (g·cm^{-3})	1.281
F**(000)**	7168
μ (mm^{-1})	2.007
crystal size, mm^3	0.18×0.12×0.11
transmission factors	0.6296 – 0.7456
θ **range (deg)**	2.594 – 25.000
data/restraints/param	7965/400/402
GOF	1.021
R_1 [I > 2σ(I)]	0.0400
wR_2 [all data]	0.0961
residual density, e/Å^3	0.642 and -0.364

Computational Details

All the calculations were conducted using the Gaussian09 program suite.[6] For all calculations the B3PW91[7] functional was used in combination with the SDD basis set and corresponding ECP for Ni,[8] and 6-31G** for all other atoms. The stationary point was confirmed as an energy minimum by the lack of imaginary frequencies.

Table S5. Coordinates for the calculated structure of complex cation 2

Br	9.103000	9.440000	8.268000
C	7.839000	10.002000	4.326000
C	8.756000	9.885000	3.211000
C	8.348000	10.048000	1.862000
C	6.927000	10.409000	1.480000
C	6.013000	10.544000	2.682000
C	6.464000	10.324000	4.009000
C	6.954000	11.762000	0.717000
H	7.345000	12.562000	1.350000
H	5.950000	12.044000	0.389000
H	7.583000	11.691000	-0.174000
C	6.359000	9.299000	0.554000
H	6.969000	9.193000	-0.346000
H	5.342000	9.543000	0.237000
H	6.335000	8.334000	1.068000
C	10.112000	9.567000	3.504000

C	11.032000	9.377000	2.485000
H	12.061000	9.110000	2.701000
C	10.620000	9.531000	1.157000
H	11.334000	9.389000	0.350000
C	9.305000	9.866000	0.858000
H	9.024000	9.981000	-0.184000
C	11.648000	10.742000	5.778000
H	11.768000	10.559000	6.854000
C	11.010000	12.123000	5.597000
H	11.689000	12.894000	5.975000
H	10.068000	12.208000	6.147000
H	10.816000	12.341000	4.541000
C	13.011000	10.653000	5.089000
H	12.937000	10.893000	4.024000
H	13.480000	9.671000	5.193000
H	13.690000	11.386000	5.538000
C	11.276000	7.761000	5.478000
H	12.043000	7.748000	4.692000
C	11.959000	7.577000	6.836000
H	11.235000	7.617000	7.653000
H	12.728000	8.331000	7.027000
H	12.448000	6.598000	6.857000

C	10.269000	6.641000	5.198000
H	10.784000	5.675000	5.204000
H	9.781000	6.751000	4.225000
H	9.497000	6.612000	5.973000
C	5.550000	10.448000	5.093000
C	4.233000	10.816000	4.871000
H	3.537000	10.935000	5.696000
C	3.797000	11.039000	3.561000
H	2.766000	11.323000	3.374000
C	4.674000	10.898000	2.491000
H	4.299000	11.075000	1.488000
C	5.880000	11.592000	7.757000
H	4.807000	11.751000	7.577000
C	6.100000	11.364000	9.255000
H	7.151000	11.166000	9.475000
H	5.508000	10.533000	9.648000
H	5.799000	12.266000	9.798000
C	6.647000	12.819000	7.254000
H	6.311000	13.709000	7.795000
H	6.492000	13.001000	6.186000
H	7.721000	12.703000	7.435000
C	5.495000	8.613000	7.447000

H	6.022000	8.509000	8.405000
C	5.804000	7.377000	6.597000
H	5.397000	6.484000	7.083000
H	6.881000	7.230000	6.475000
H	5.349000	7.449000	5.602000
C	3.994000	8.764000	7.703000
H	3.431000	8.805000	6.765000
H	3.747000	9.649000	8.296000
H	3.633000	7.891000	8.257000
Ni	8.402000	9.751000	6.080000
P	10.435000	9.416000	5.295000
P	6.321000	10.110000	6.714000

Table S6. Coordinates for the calculated structure of II

C	5.47799	7.56459	13.81071
C	5.47566	8.95526	14.16866
C	6.67829	9.71991	14.32745
C	8.00787	8.96809	14.38726
C	7.96283	7.77269	13.43758
C	6.72709	7.05588	13.31618
C	8.14156	8.39898	15.82630
H	8.15208	9.21397	16.55942
H	9.06817	7.82120	15.92350

H	7.29884	7.73982	16.05537
C	9.21153	9.88048	14.12592
H	9.17847	10.31914	13.12326
H	10.14981	9.32830	14.23166
H	9.25305	10.69237	14.85761
C	4.24523	9.63608	14.37912
C	4.17888	10.99538	14.68428
H	3.22127	11.47490	14.87377
C	5.35108	11.74103	14.74534
H	5.32379	12.80578	14.95670
C	6.57916	11.08440	14.57034
H	7.48647	11.67462	14.66304
C	1.65642	9.05030	12.98394
H	0.91348	8.24119	12.94035
C	2.35400	9.13671	11.62326
H	1.62869	9.38189	10.83863
H	2.84292	8.19349	11.36463
H	3.12382	9.91475	11.63210
C	0.93734	10.36182	13.30939
H	1.64099	11.19927	13.31926
H	0.41880	10.33932	14.27267
H	0.18751	10.57456	12.53783

C	2.00329	8.61400	15.90941
H	1.79237	9.68526	16.03193
C	0.68364	7.84295	15.96053
H	0.86107	6.76879	15.84979
H	-0.01897	8.15512	15.18134
H	0.19378	7.99970	16.92885
C	2.94445	8.18104	17.03711
H	2.46785	8.34548	18.01078
H	3.88016	8.74539	17.01387
H	3.19303	7.11764	16.95413
C	6.77142	5.80586	12.64166
C	7.92265	5.32523	12.01831
H	7.90658	4.38148	11.47727
C	9.09080	6.07846	12.06625
H	9.99613	5.73468	11.57507
C	9.08947	7.28174	12.78941
H	10.02048	7.83842	12.84793
C	4.76559	4.58803	10.90322
H	5.59437	3.93544	10.59597
C	3.45405	3.81542	10.75692
H	2.60431	4.43410	11.06401
H	3.43991	2.89597	11.35099

H	3.29845	3.53317	9.70898
C	4.78415	5.82992	10.00919
H	4.65935	5.53894	8.95956
H	5.72442	6.37872	10.10449
H	3.96895	6.51222	10.26933
C	5.24085	3.43936	13.60412
H	4.20417	3.07340	13.61723
C	5.66859	3.72297	15.04816
H	5.65153	2.79864	15.63766
H	5.01226	4.45565	15.52724
H	6.68606	4.12537	15.07681
C	6.13361	2.37351	12.96587
H	7.17569	2.70598	12.93681
H	5.82725	2.11628	11.94711
H	6.09947	1.45270	13.56066
C	1.42664	4.76664	13.88368
C	0.25397	3.88570	14.02370
C	-0.98987	4.63857	13.51124
H	-1.16496	5.55187	14.08609
H	-1.86787	3.99330	13.61560
H	-0.88411	4.90690	12.45642
C	0.08480	3.52345	15.51312

H	0.96572	3.00135	15.89646
H	-0.78218	2.86453	15.62525
H	-0.08146	4.41509	16.12343
C	0.48522	2.60985	13.19150
H	0.61619	2.84323	12.13173
H	-0.38510	1.95418	13.29461
H	1.36717	2.06426	13.53829
N	2.34788	5.47145	13.78768
Ni	3.87473	6.56591	13.68522
P	2.88995	8.46579	14.26773
P	5.14147	5.06206	12.67267

Table S7. Coordinates for the calculated structure of 2_{red}

Br	6.76581	5.03990	3.89493
C	2.78440	3.87434	2.93181
C	2.44461	2.49964	2.64991
C	1.12502	2.07007	2.34069
C	-0.04601	3.04593	2.24523
C	0.37006	4.48602	2.53797
C	1.70750	4.83425	2.87176
C	3.47864	1.52399	2.70445
C	3.21989	0.17419	2.49714
H	4.01591	-0.56140	2.57132

C	1.92065	-0.23831	2.20020
H	1.70113	-1.28884	2.03289
C	0.90076	0.71025	2.12050
H	-0.10345	0.36692	1.88519
C	2.00437	6.19942	3.14067
C	1.03205	7.18873	3.05237
H	1.28191	8.23047	3.23301
C	-0.27632	6.83782	2.71859
H	-1.04915	7.59773	2.64747
C	-0.58694	5.49990	2.47411
H	-1.61305	5.24882	2.21769
C	-1.13102	2.62850	3.26779
H	-1.48165	1.60958	3.07797
H	-1.99830	3.29351	3.21401
H	-0.73563	2.66772	4.28705
C	-0.63052	2.97506	0.81319
H	0.12076	3.27109	0.07514
H	-1.49329	3.63930	0.70544
H	-0.96070	1.95975	0.57350
C	6.25264	1.97140	1.69283
H	7.17591	2.45279	2.04161
C	5.76114	2.72887	0.45577

H	6.48643	2.62554	-0.35928
H	5.63495	3.79452	0.66728
H	4.80138	2.33486	0.10417
C	6.52900	0.50123	1.37328
H	5.63614	0.00962	0.97423
H	6.87404	-0.06625	2.24297
H	7.30934	0.43151	0.60652
C	5.71384	1.26912	4.55278
H	5.55978	0.21999	4.26334
C	7.19917	1.49077	4.84812
H	7.40032	2.54068	5.07686
H	7.84009	1.20209	4.00988
H	7.49247	0.88308	5.71219
C	4.85153	1.56184	5.78468
H	5.14303	0.90252	6.61017
H	3.78668	1.40556	5.58725
H	4.99115	2.59660	6.11337
C	4.32642	7.78702	2.38966
H	3.55172	8.56410	2.45381
C	5.67564	8.39621	2.77837
H	6.45959	7.63440	2.79222
H	5.65207	8.87038	3.76397

H	5.95050	9.16650	2.04829
C	4.35105	7.24748	0.95607
H	4.57802	8.05894	0.25527
H	3.39153	6.80887	0.66586
H	5.12513	6.48116	0.84760
C	3.88430	7.11578	5.27342
H	4.96885	7.22382	5.40726
C	3.38520	6.06785	6.27259
H	3.53140	6.42791	7.29730
H	3.92735	5.12446	6.16171
H	2.31723	5.86578	6.13606
C	3.20220	8.46689	5.49478
H	2.11404	8.37646	5.41860
H	3.53375	9.23260	4.78684
H	3.42885	8.83308	6.50288
Ni	4.55591	4.39276	3.36042
P	5.08189	2.27689	3.11208
P	3.76171	6.43018	3.54326

NMR Spectra

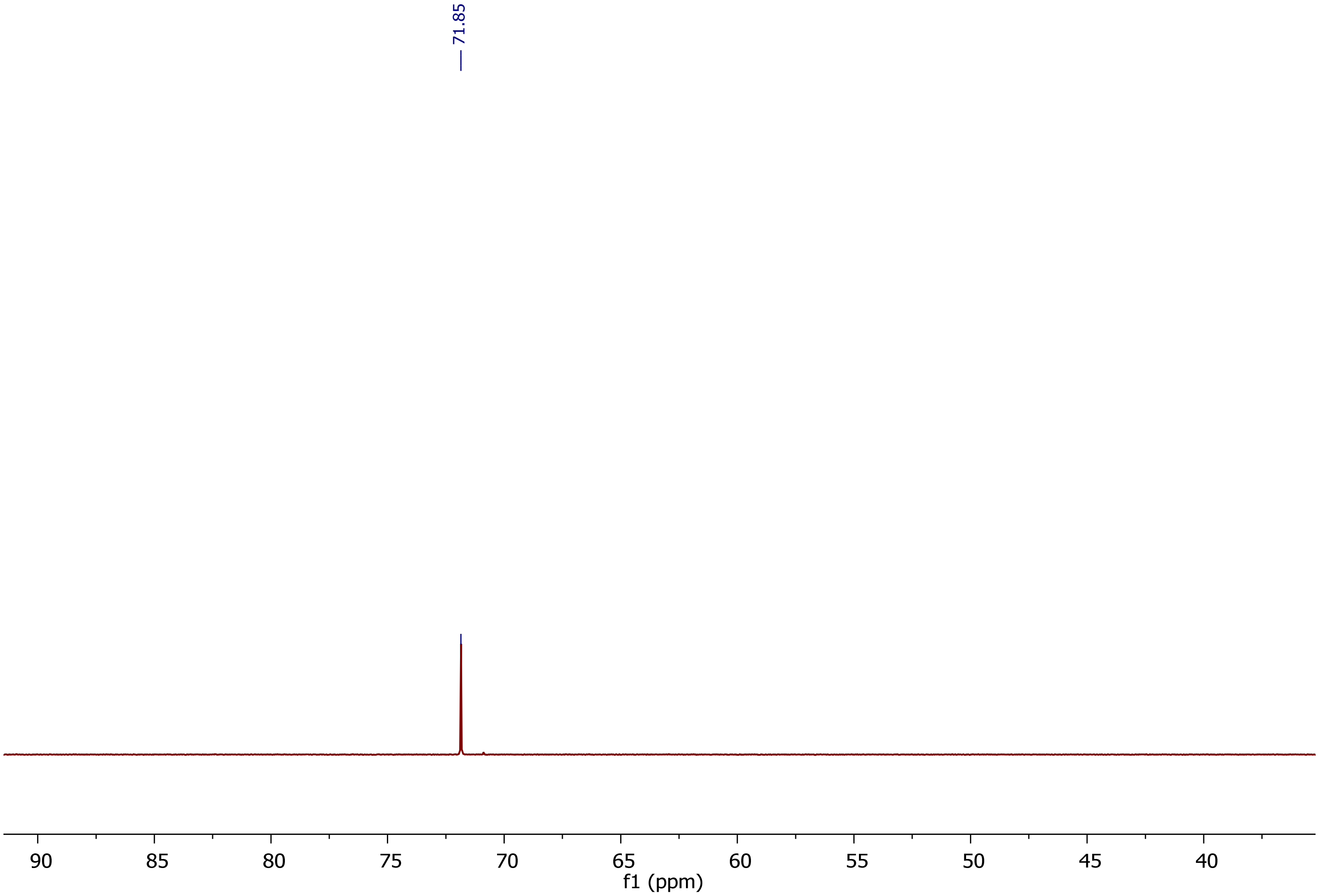

Figure S10: $^{31}P\{^{1}H\}$ NMR Spectrum of Complex 2

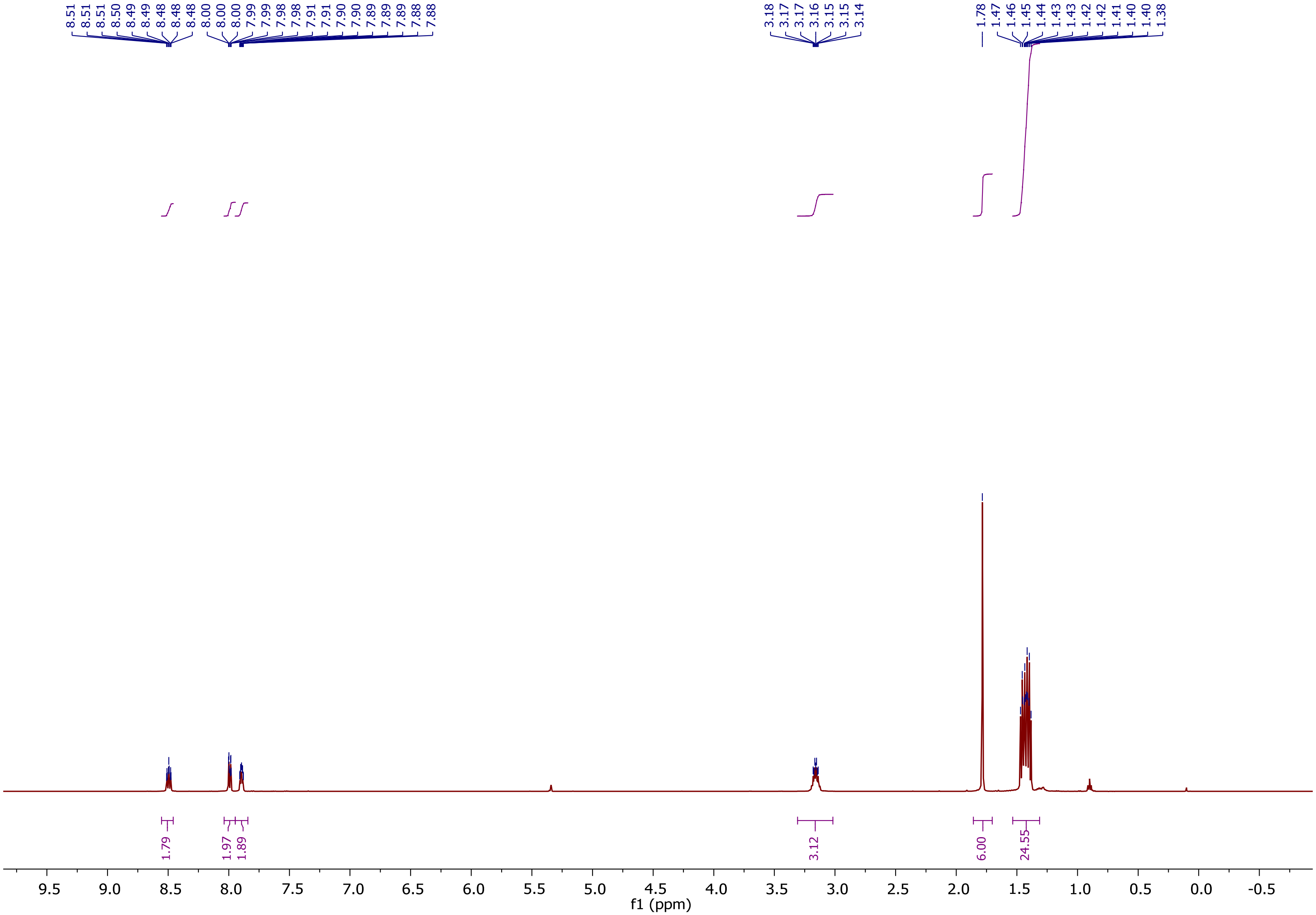

Figure S11: ^{1}H NMR Spectrum of Complex 2

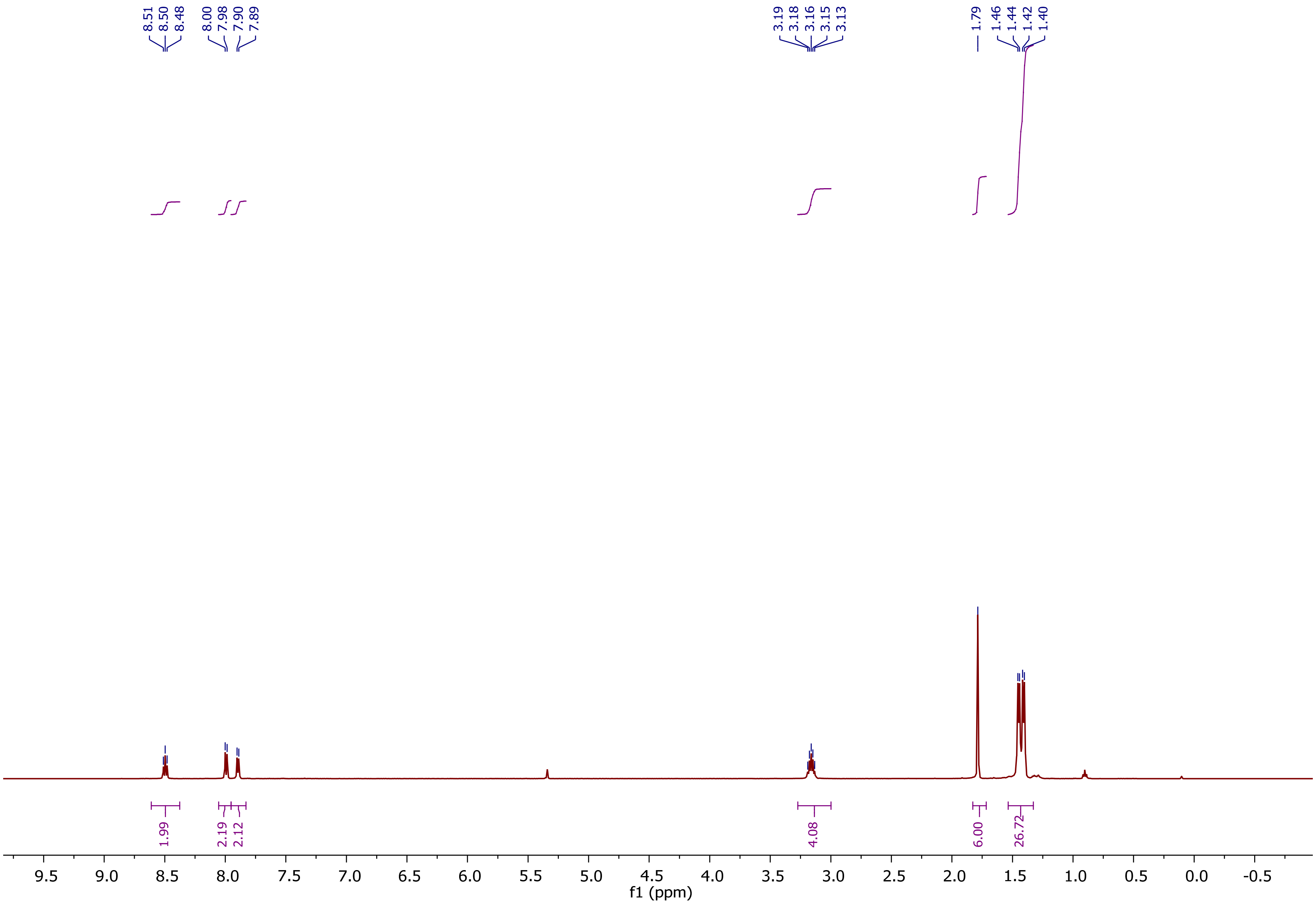

Figure S12: $^{1}H\{^{31}P\}$ NMR Spectrum of Complex 2

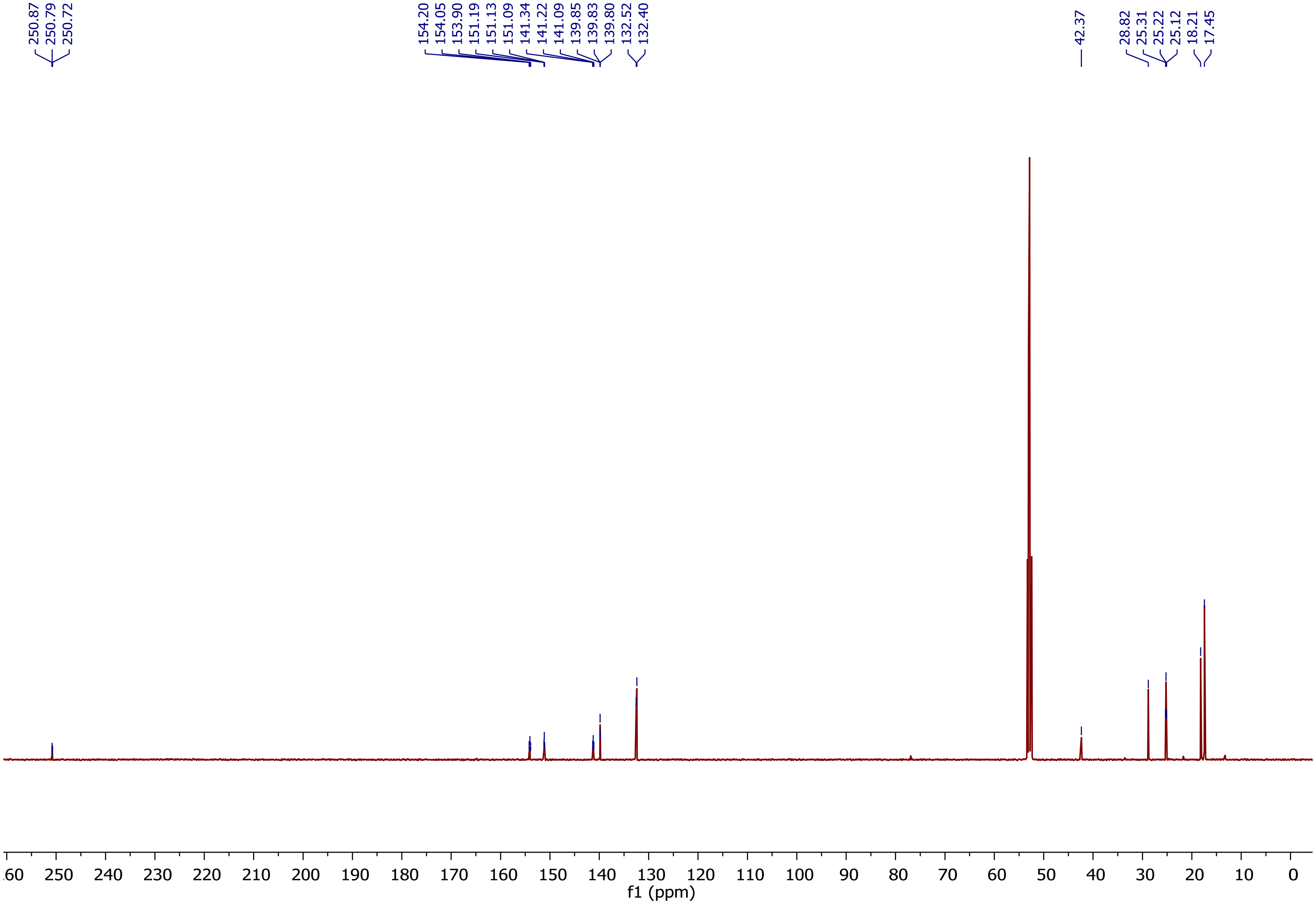

Figure S13: $^{13}C\{^1H\}$ NMR Spectrum of Complex 2

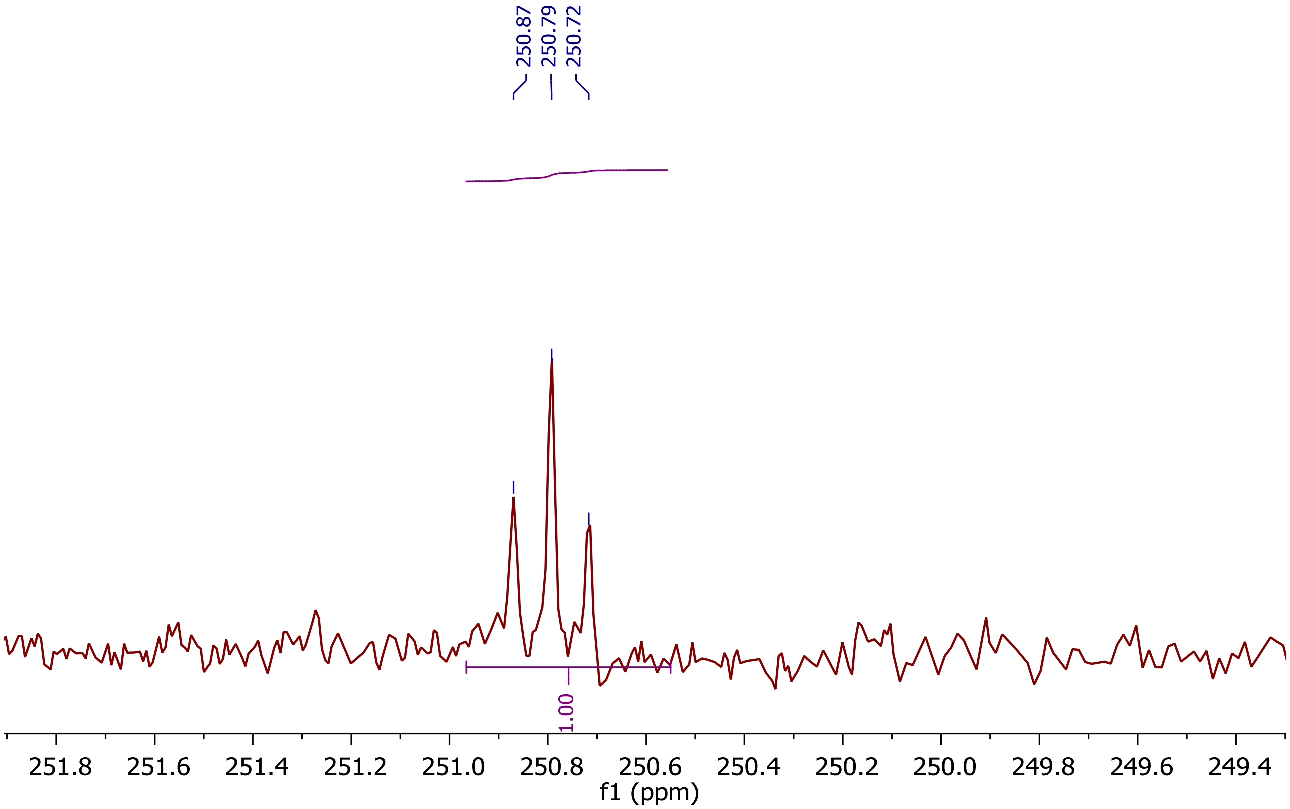

Figure S14: $^{13}C\{^{1}H\}$ NMR Spectrum of Complex 2 (Highlight of Carbene Peak)

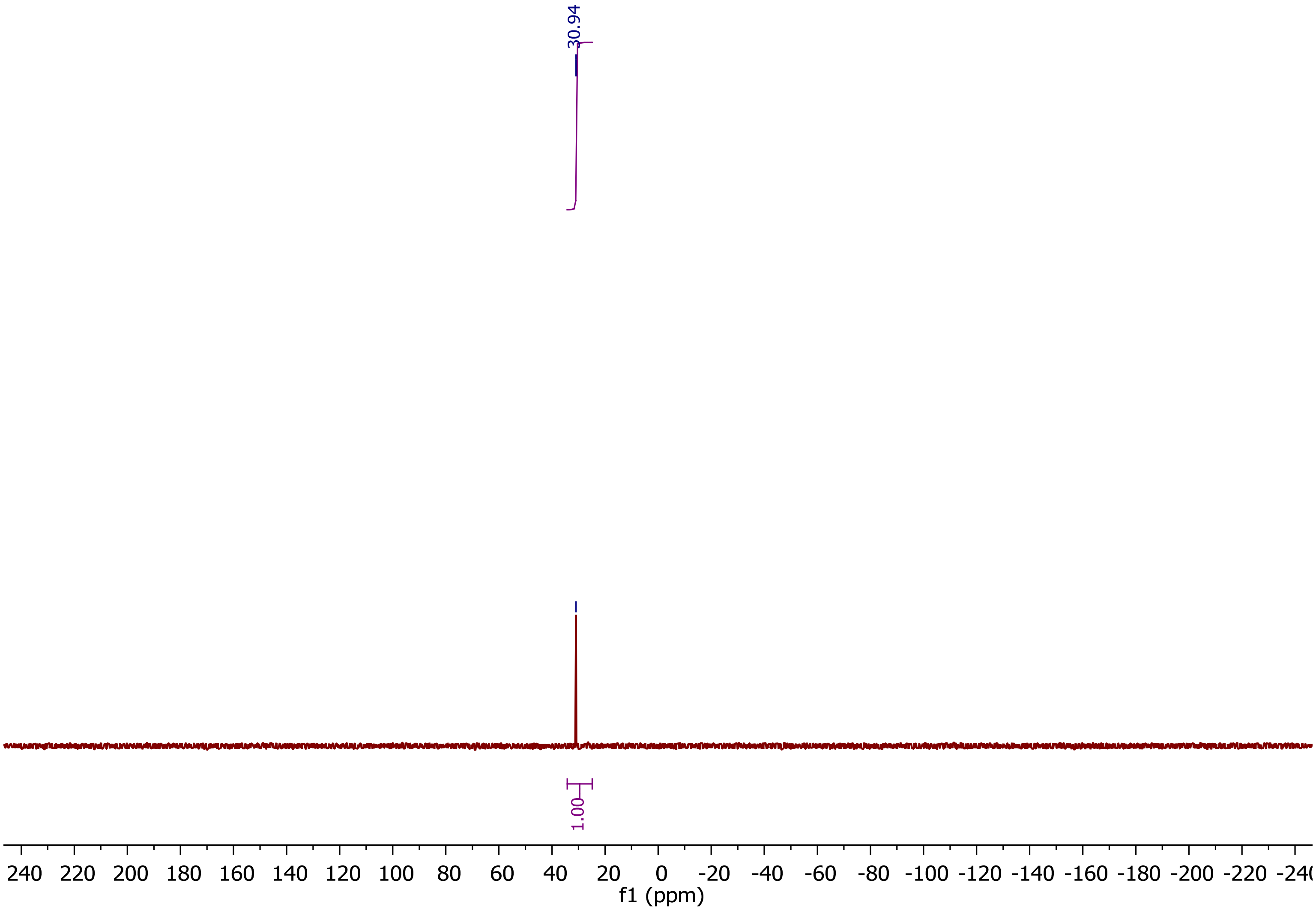

Figure S15: $^{31}P\{^1H\}$ NMR Spectrum of Complex 3_O

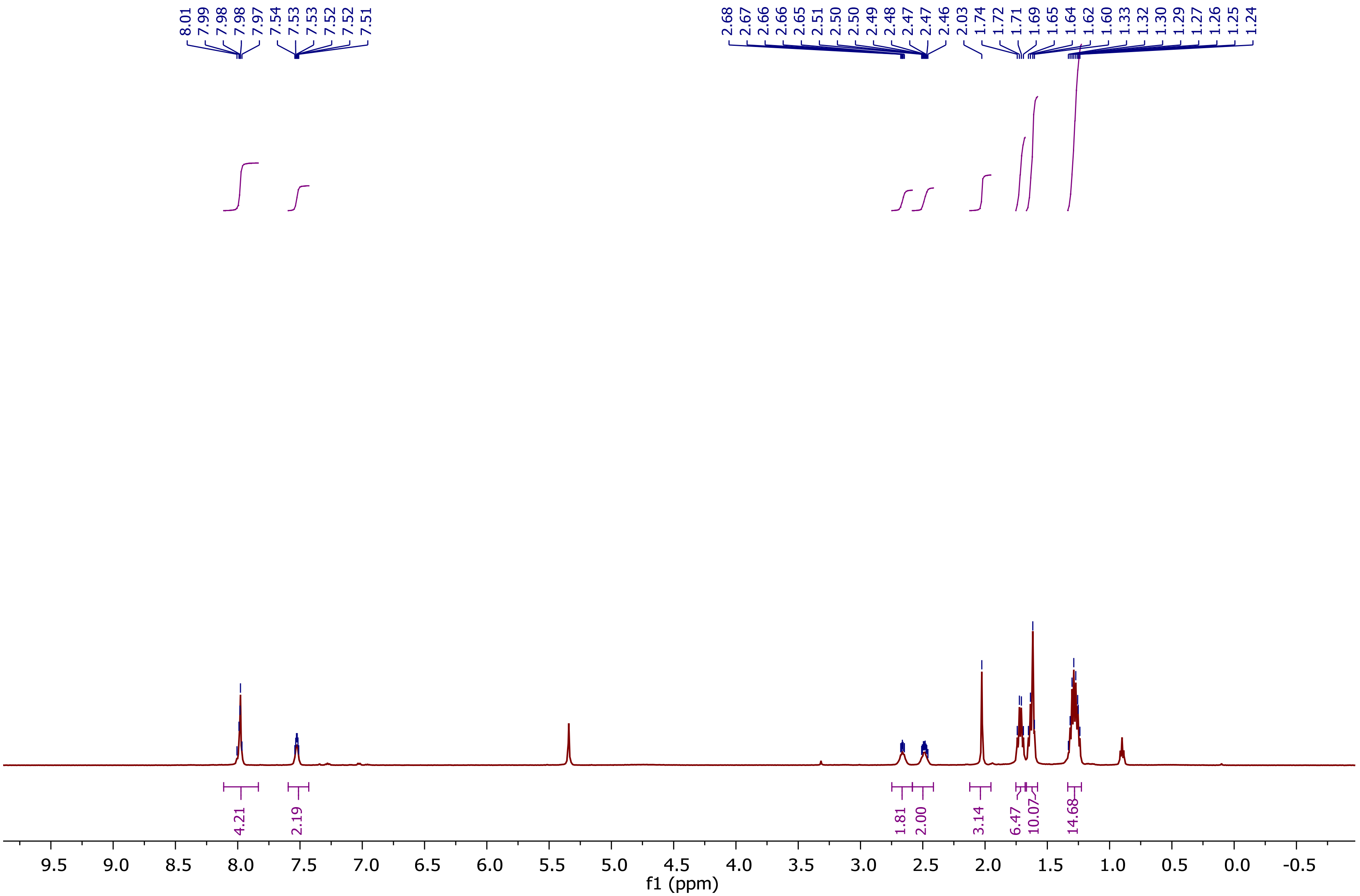

Figure S16: ^{1}H NMR Spectrum of Complex 3_O (Trace Contamination from $NMePh_2$ Evident)

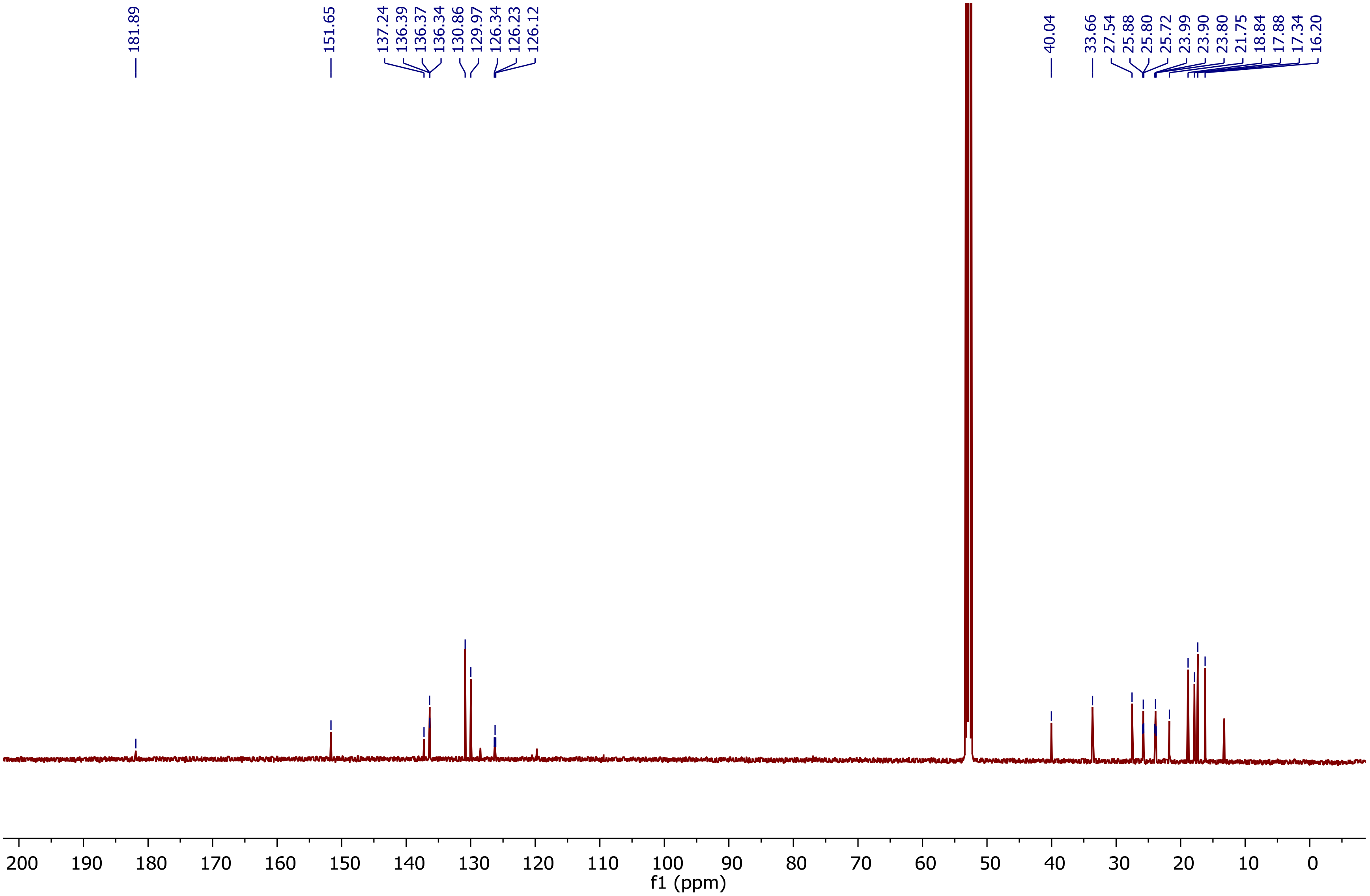

Figure S17: $^{13}C\{^{1}H\}$ **NMR Spectrum of Complex** 3_{O} **(Trace Contamination from** $NMePh_2$ **Evident)**

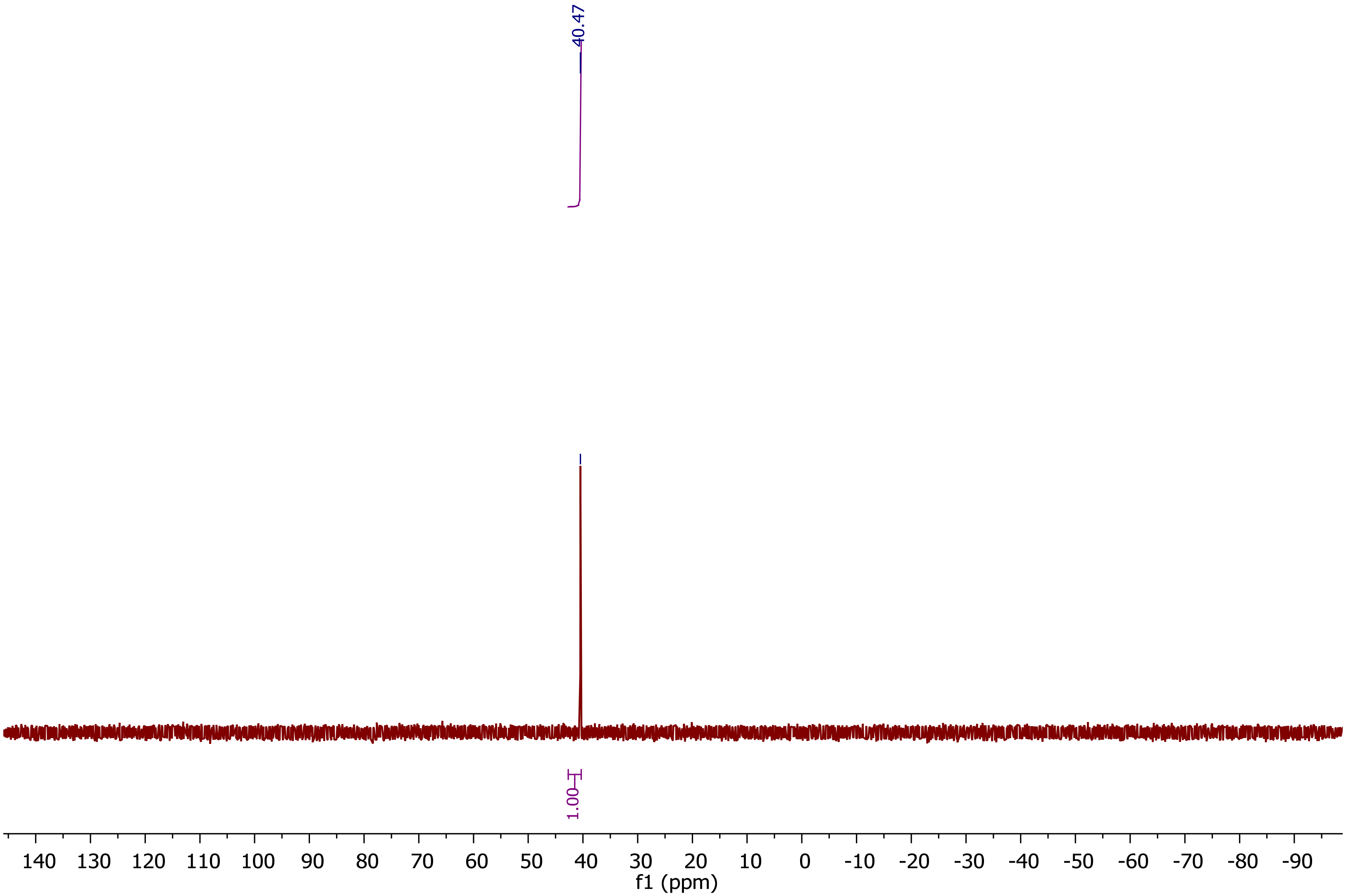

Figure S18: $^{31}P\{^1H\}$ **NMR Spectrum of Complex** 3_{NTs}

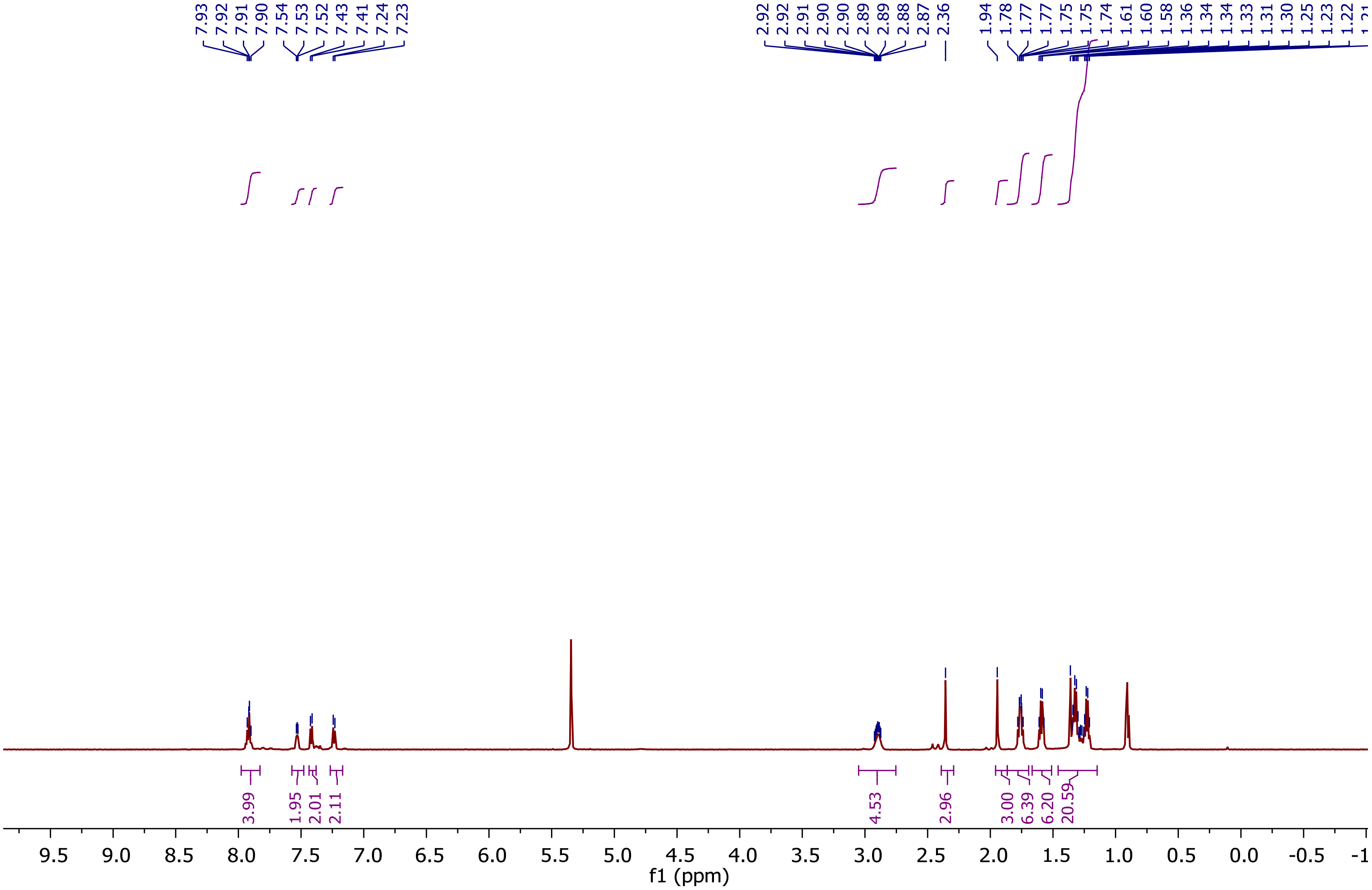

Figure S19: ^{1}H NMR Spectrum of Complex 3_{NTs} (Contamination by *n*-pentane observable)

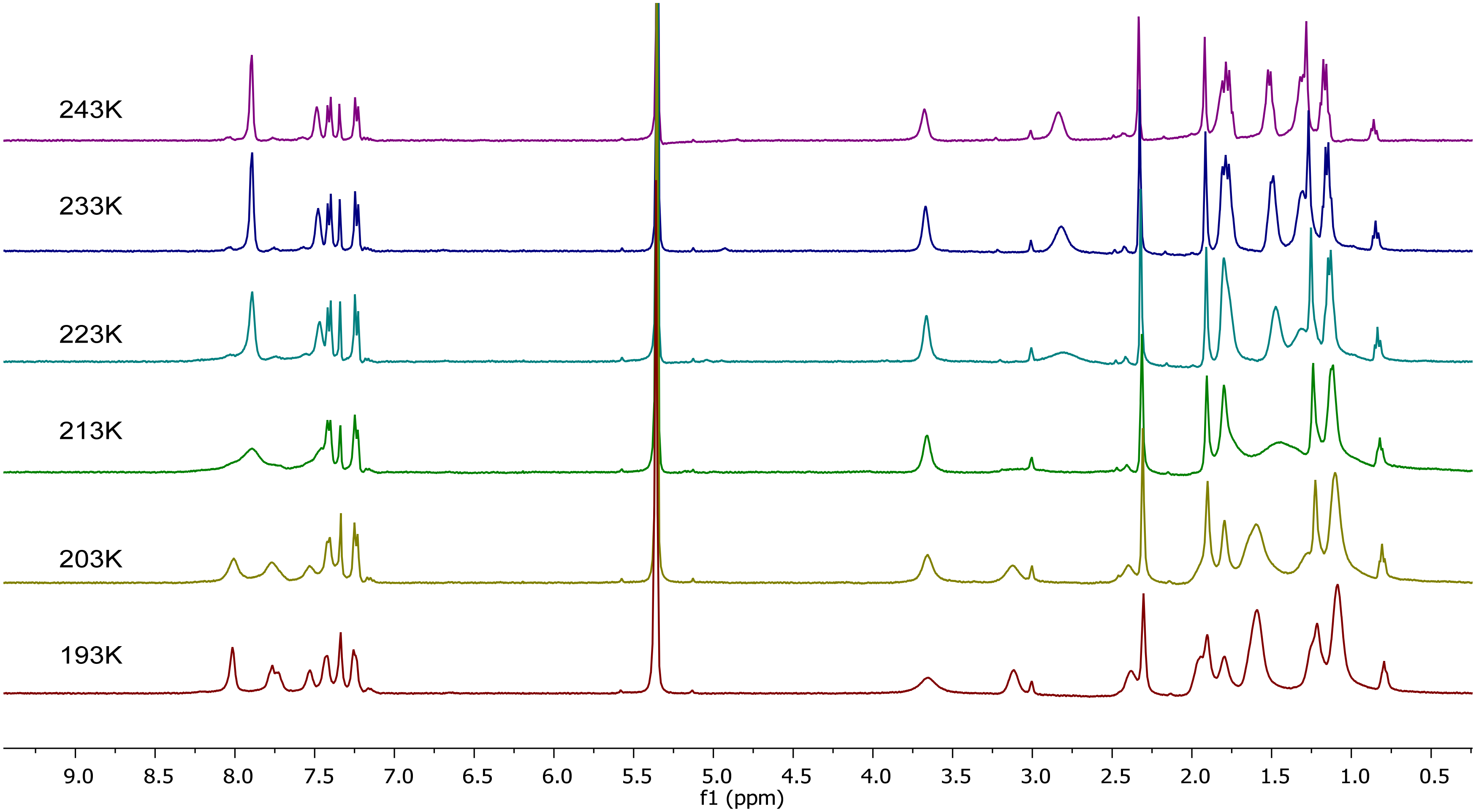

Figure S20: Variable Temperature ^{1}H NMR Spectrum of Complex 3_{NTs}

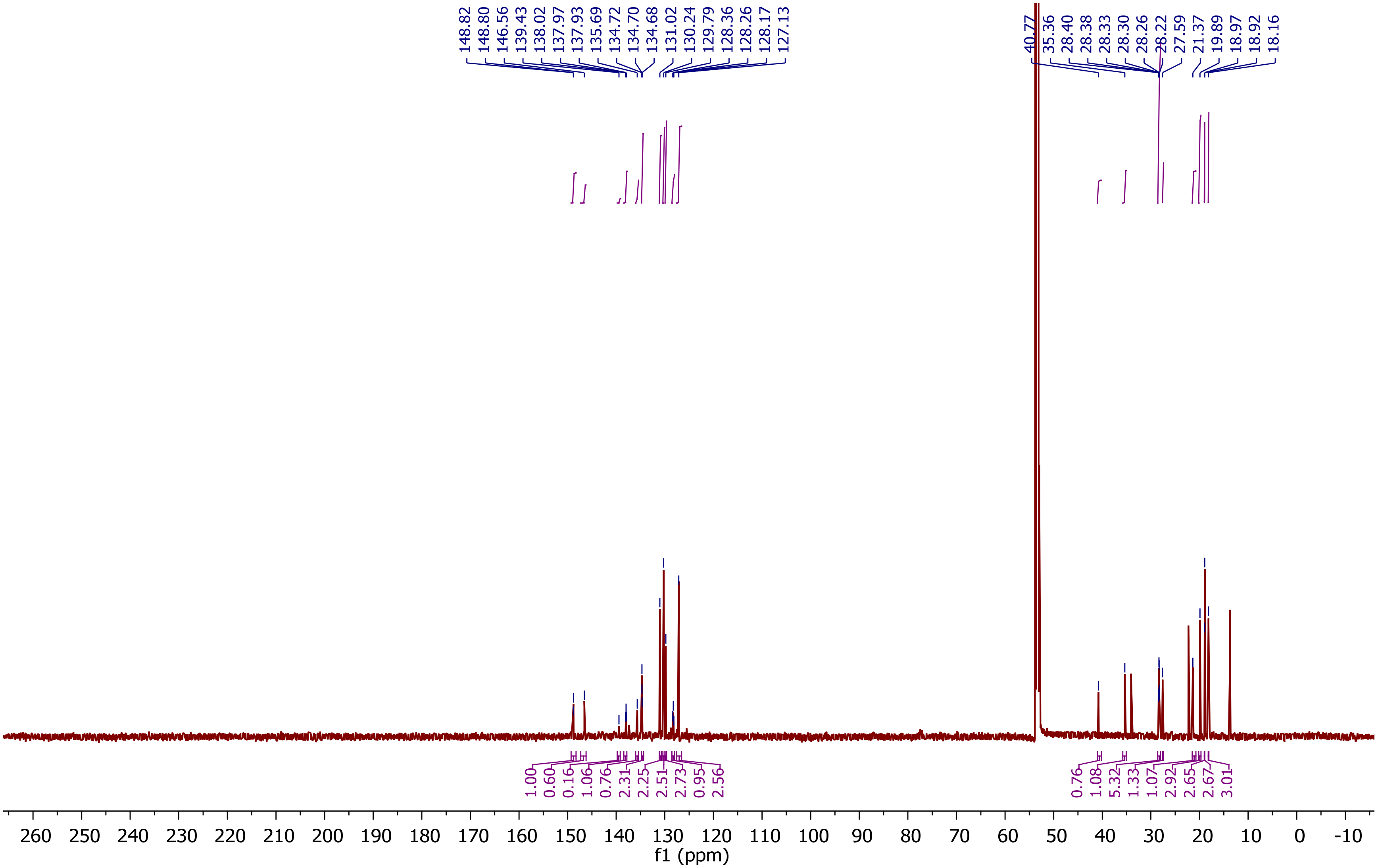

Figure S21: $^{13}C\{^{1}H\}$ **NMR Spectrum of Complex** 3_{NTs} **(Contamination by *n*-pentane observable)**

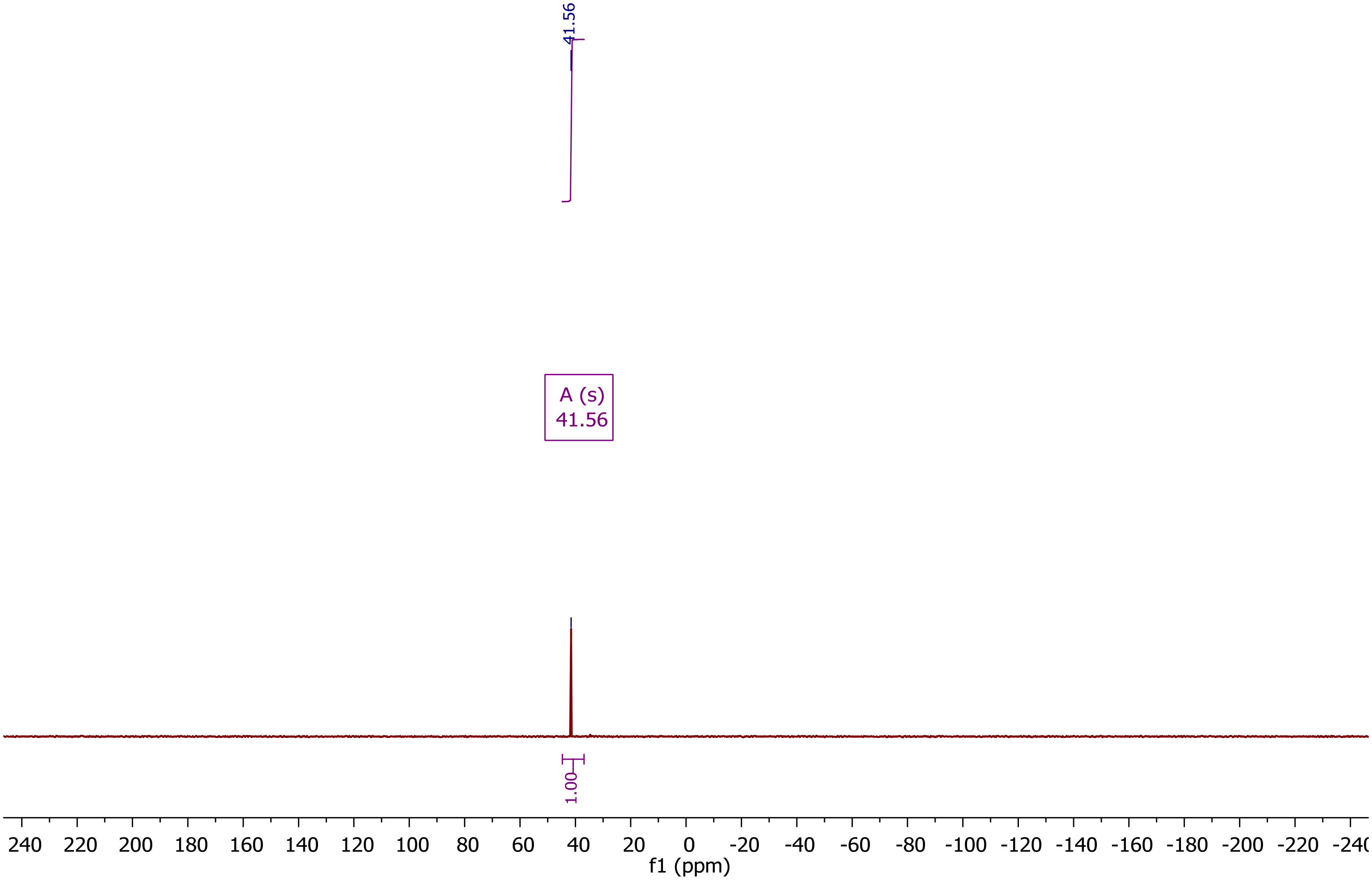

Figure S22: $^{31}P\{^{1}H\}$ **NMR Spectrum of Complex 4**

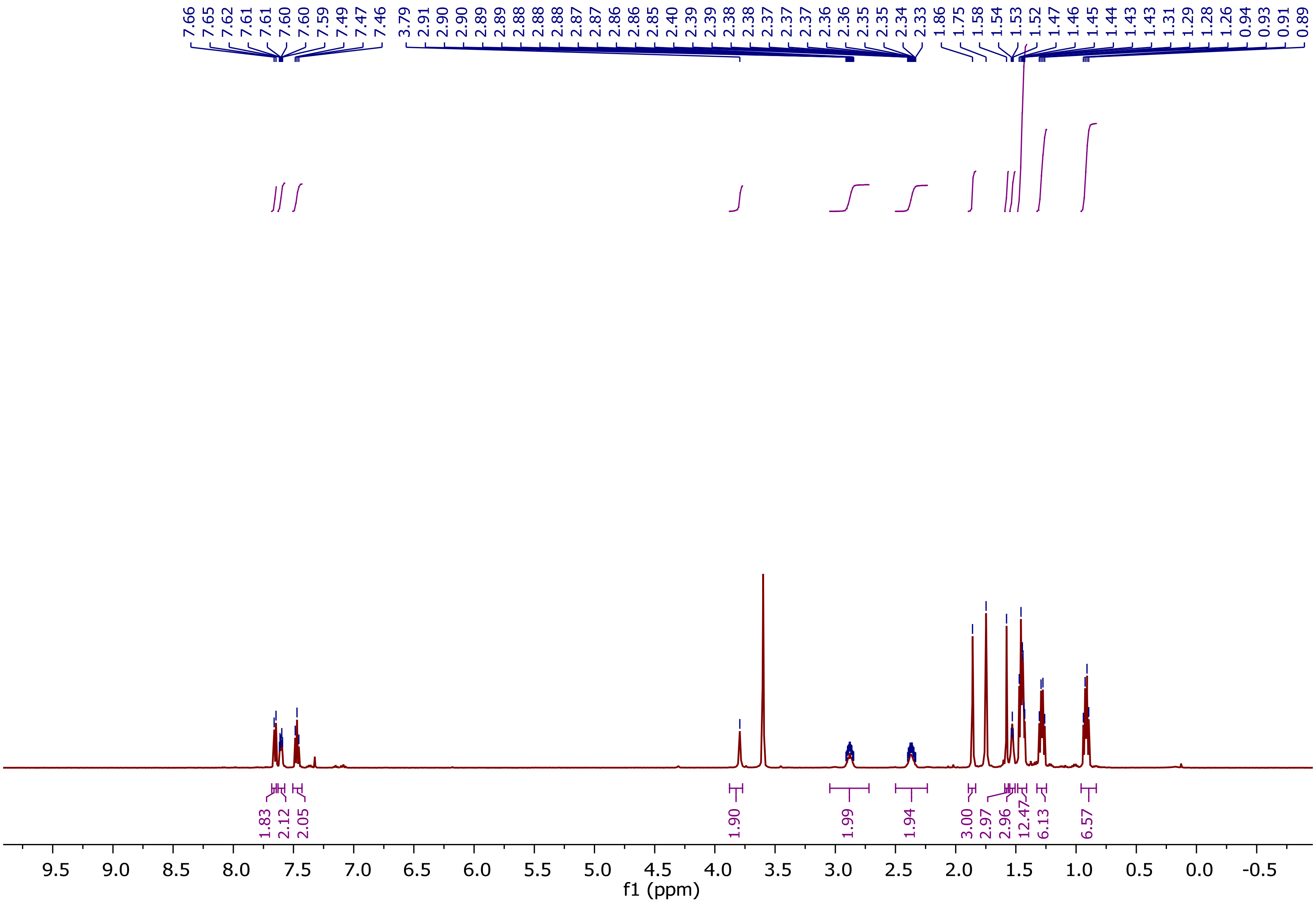

Figure S23: ^{1}H NMR Spectrum of Complex 4

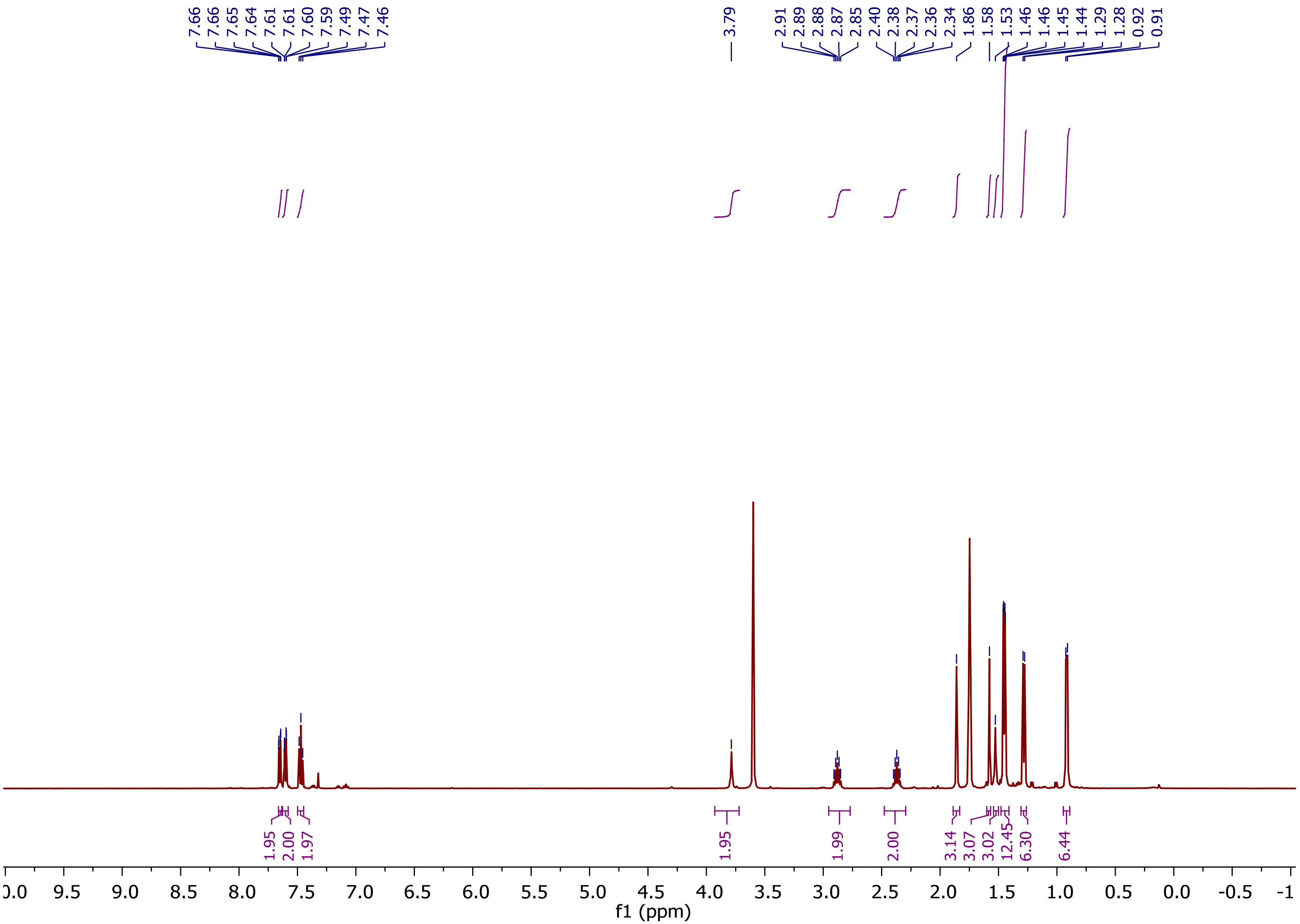

Figure S24: $^{1}H\{^{31}P\}$ NMR Spectrum of Complex 4

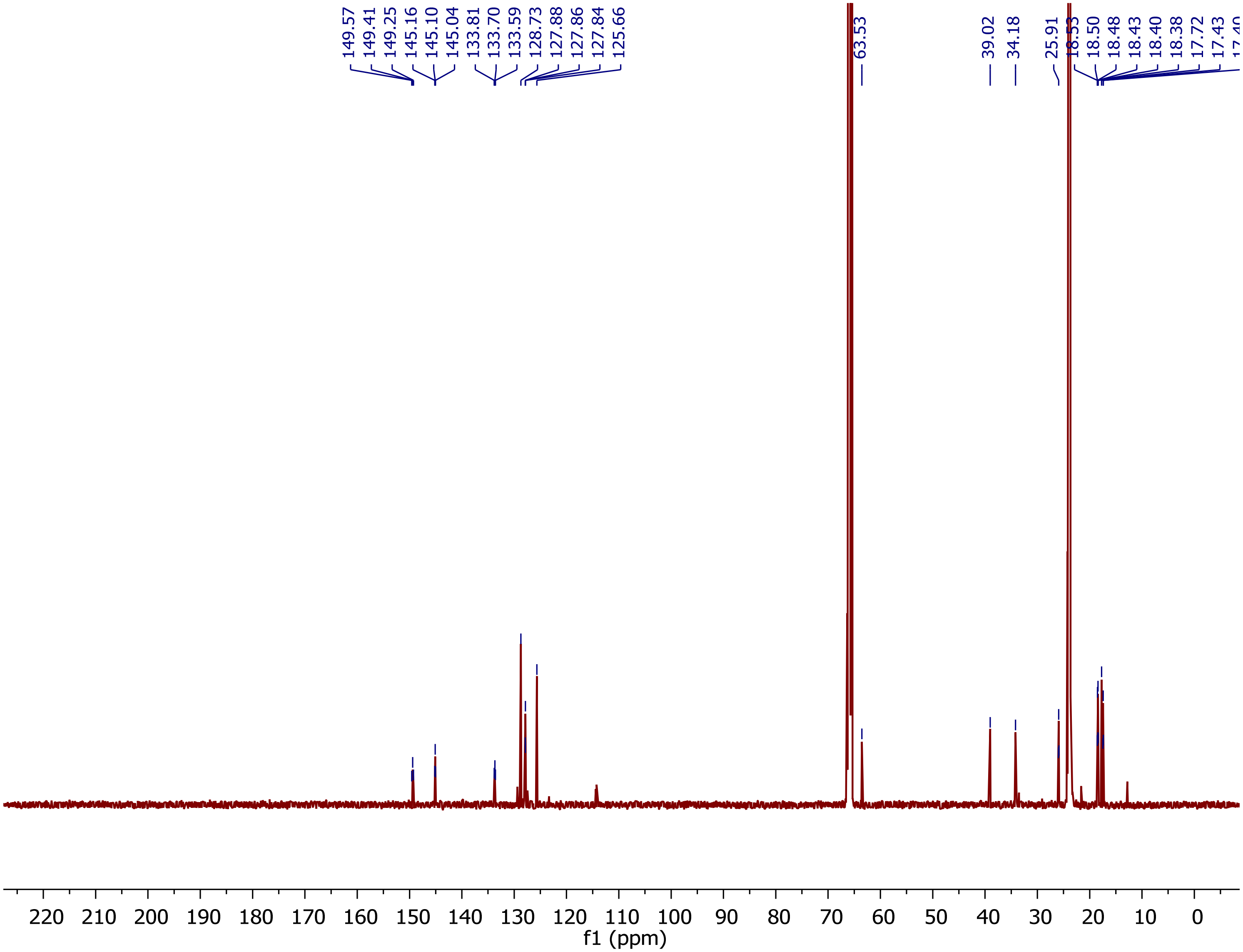

Figure S25: $^{13}C\{^{1}H\}$ NMR Spectrum of Complex 4

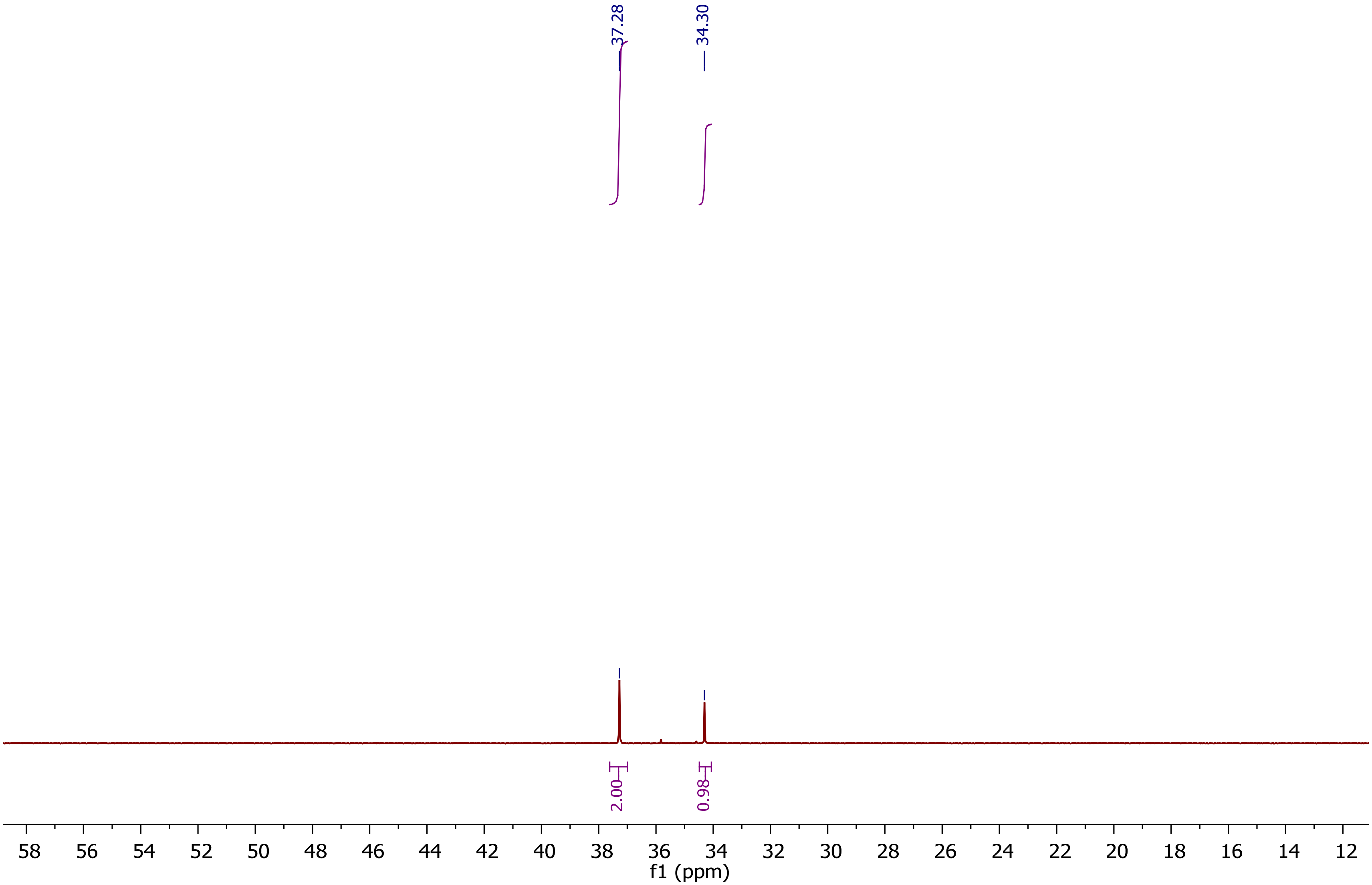

Figure S26: $^{31}P\{^{1}H\}$ NMR Spectrum of Complex 5

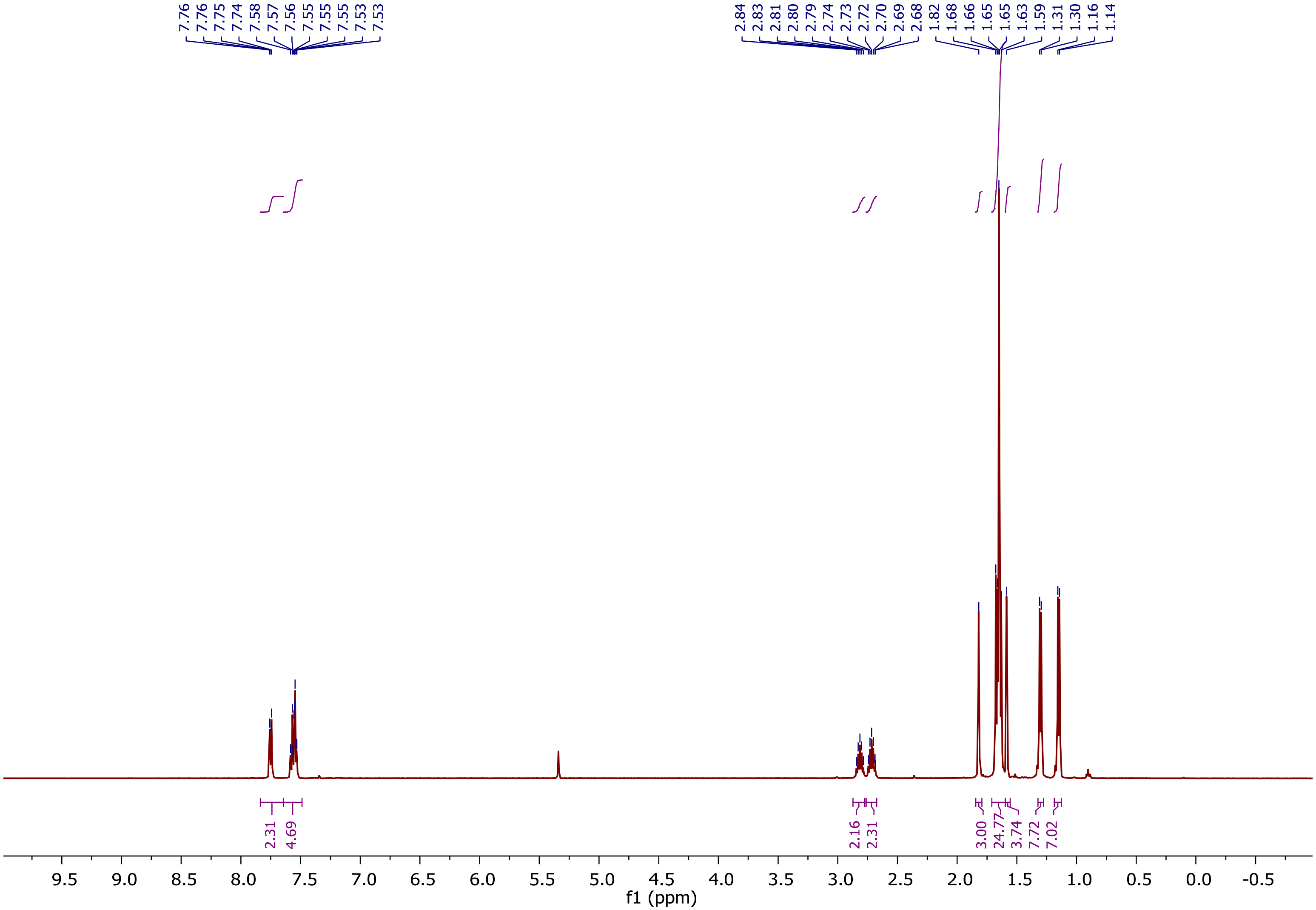

Figure S27: ^{1}H NMR Spectrum of Complex 6

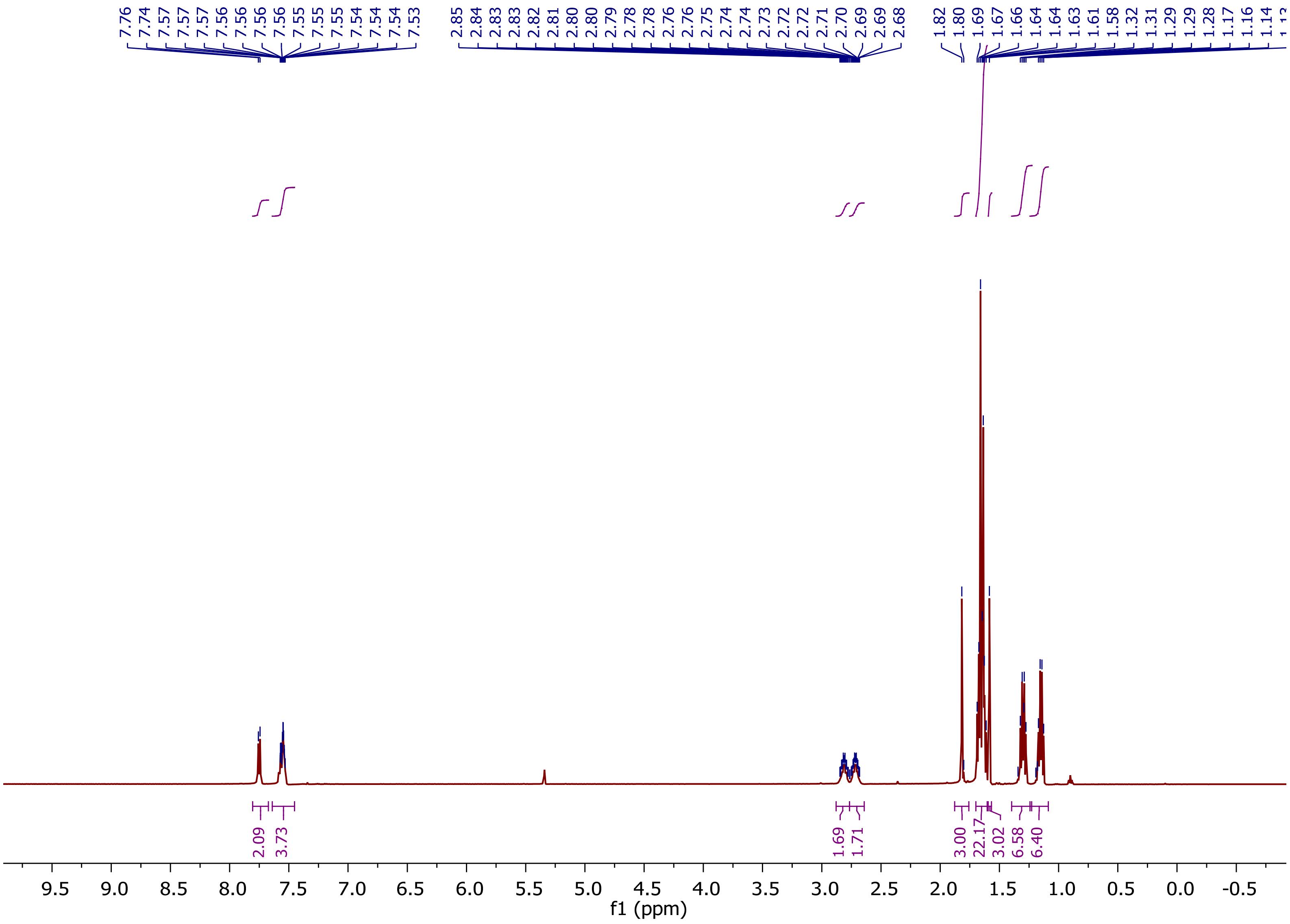

Figure S28: $^{1}H\{^{31}P\}$ NMR Spectrum of Complex 6

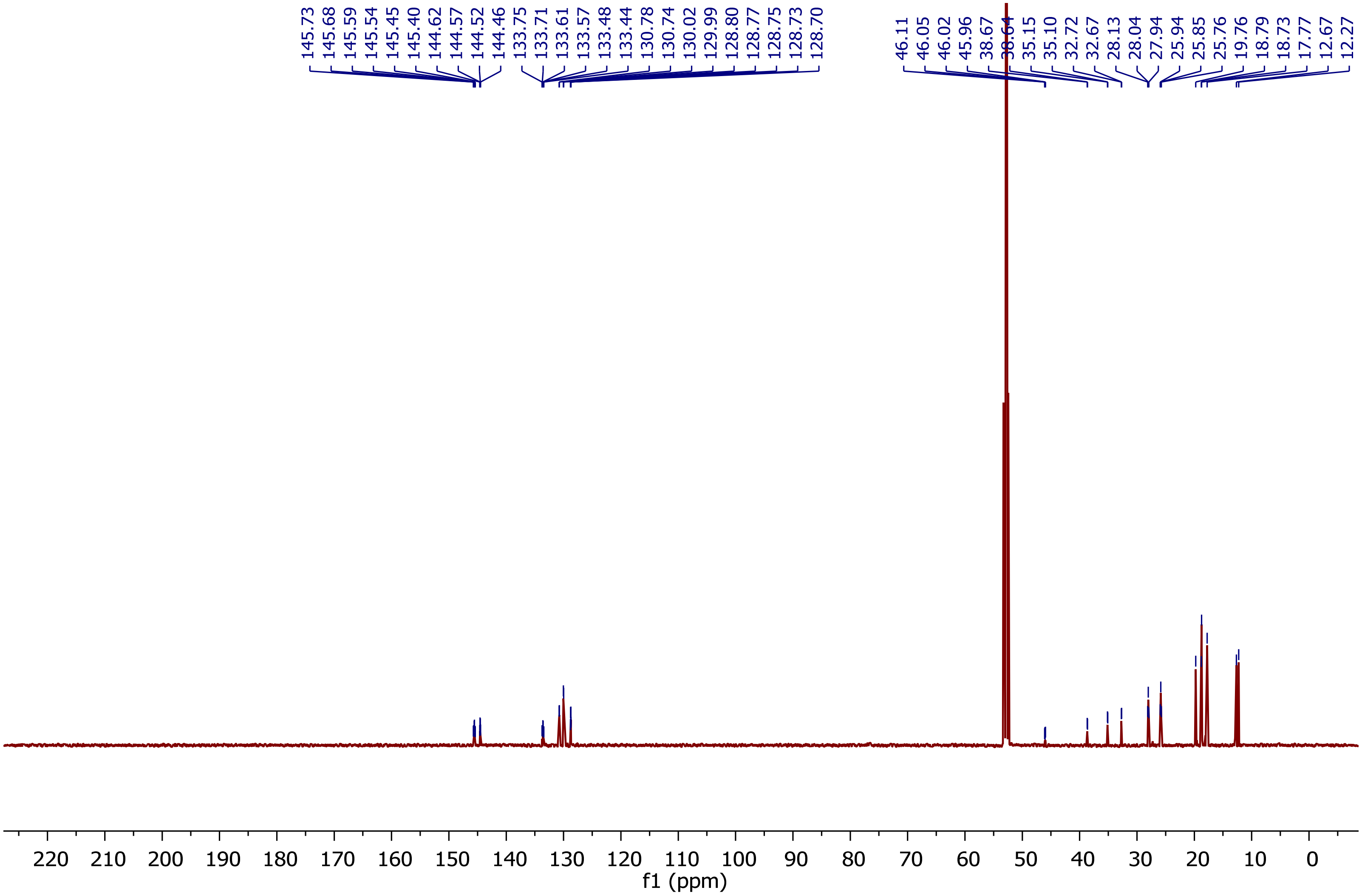

Figure S29: $^{13}C\{^1H\}$ **NMR Spectrum of Complex 6**

References

1. E. A. LaPierre, W. E. Piers and C. Gendy, *Organometallics*, 2018, DOI: 10.1021/acs.organomet.8b00440.
2. A. Yoshimura, M. W. Luedtke and V. V. Zhdankin, *The Journal of Organic Chemistry*, 2012, **77**, 2087-2091.
3. E. A. LaPierre, M. L. Clapson, W. E. Piers, L. Maron, D. M. Spasyuk and C. Gendy, *Inorg Chem*, 2018, **57**, 495-506.
4. C. Douvris and O. V. Ozerov, *Science*, 2008, **321**, 1188.
5. V. J. Scott, R. Çelenligil-Çetin and O. V. Ozerov, *Journal of the American Chemical Society*, 2005, **127**, 2852-2853.
6. Gaussian 09, Revision C.01, M. J. Frisch, G. W. Trucks, H. B. Schlegel, G. E. Scuseria, M. A. Robb, J. R. Cheeseman, G. Scalmani, V. Barone, G. A. Petersson, H. Nakatsuji, X. Li, M. Caricato, A. Marenich, J. Bloino, B. G. Janesko, R. Gomperts, B. Mennucci, H. P. Hratchian, J. V. Ortiz, A. F. Izmaylov, J. L. Sonnenberg, D. Williams-Young, F. Ding, F. Lipparini, F. Egidi, J. Goings, B. Peng, A. Petrone, T. Henderson, D. Ranasinghe, V. G. Zakrzewski, J. Gao, N. Rega, G. Zheng, W. Liang, M. Hada, M. Ehara, K. Toyota, R. Fukuda, J. Hasegawa, M. Ishida, T. Nakajima, Y. Honda, O. Kitao, H. Nakai, T. Vreven, K. Throssell, J. A. Montgomery, Jr., J. E. Peralta, F. Ogliaro, M. Bearpark, J. J. Heyd, E. Brothers, K. N. Kudin, V. N. Staroverov, T. Keith, R. Kobayashi, J. Normand, K. Raghavachari, A. Rendell, J. C. Burant, S. S. Iyengar, J. Tomasi, M. Cossi, J. M. Millam, M. Klene, C. Adamo, R. Cammi, J. W. Ochterski, R. L. Martin, K. Morokuma, O. Farkas, J. B. Foresman, and D. J. Fox, Gaussian, Inc., Wallingford CT, 2016.
7. J. P. Perdew and Y. Wang, *Physical Review B*, 1992, **45**, 13244-13249.
8. M. Dolg, U. Wedig, H. Stoll and H. Preuss, *The Journal of Chemical Physics*, 1987, **86**, 866-872.